

Ring1-mediated ubiquitination of H2A restrains poised RNA polymerase II at bivalent genes in mouse ES cells

Julie K. Stock^{1*}, Sara Giadrossi^{2*}, Miguel Casanova³, Emily Brookes¹, Miguel Vidal⁴, Haruhiko Koseki⁵, Neil Brockdorff³, Amanda G. Fisher^{2,6} and Ana Pombo^{1,6}

Changes in phosphorylation of the carboxy-terminal domain (CTD) of RNA polymerase II (RNAP) are associated with transcription initiation, elongation and termination^{1–3}. Sites of active transcription are generally characterized by hyperphosphorylated RNAP, particularly at Ser 2 residues, whereas inactive or poised genes may lack RNAP or may bind Ser 5-phosphorylated RNAP at promoter proximal regions. Recent studies have demonstrated that silent developmental regulator genes have an unusual histone modification profile in ES cells, being simultaneously marked with Polycomb repressor-mediated histone H3K27 methylation, and marks normally associated with gene activity^{4,5}. Contrary to the prevailing view, we show here that this important subset of developmental regulator genes, termed bivalent genes, assemble RNAP complexes phosphorylated on Ser 5 and are transcribed at low levels. We provide evidence that this poised RNAP configuration is enforced by Polycomb Repressor Complex (PRC)-mediated ubiquitination of H2A, as conditional deletion of Ring1A and Ring1B leads to the sequential loss of ubiquitination of H2A, release of poised RNAP, and subsequent gene de-repression. These observations provide an insight into the molecular mechanisms that allow ES cells to self-renew and yet retain the ability to generate multiple lineage outcomes.

Recent studies have shown that Polycomb proteins are required to silence an important subset of developmental regulator genes in both human and mouse embryonic stem (ES) cells, to ensure that expression occurs only at later stages of ontogeny or upon ES cell differentiation^{6–8}. Genome-wide⁵ and candidate-based chromatin studies⁴ suggest that these genes are enriched for histone modifications associated both with gene activity (such as acetylated histone H3 and trimethylated H3K4) and with PRC2-mediated repression (such as methylated H3K27). Collectively, these reports have encouraged a view that key genes, which are either silent or not productively expressed in ES cells, are poised for future expression

(reviewed in ref. 9). Although previous genome-based surveys showed little or no enrichment of RNAP at bivalent genes in ES cells⁸ or embryonal cells^{10–12}, the presence of high levels of promoter acetylation and H3K4me3 prompted us to re-examine this issue.

RNAP is subject to complex phosphorylation of the CTD heptad consensus repeat sequence Tyr¹-Ser²-Pro³-Thr⁴-Ser⁵-Pro⁶-Ser⁷ (refs 1–3, 13), and binding of Ser 5-phosphorylated RNAP (Ser 5P) has been detected at the promoters of inducible genes prior to their activation^{14–16}. Using a modified chromatin immunoprecipitation (ChIP) approach, optimized for use with IgM or IgG antibodies, we examined Ser 5P (4H8), Ser 2P (H5) or total RNAP (H224) binding to the promoter and coding regions of a panel of so-called ‘bivalent’ genes in ES cells (Fig. 1a). As anticipated, genes that are expressed at high levels in ES cells, such as *β-actin*, *Oct4* and *Sox2*, contained appreciable levels of Ser 5P, Ser 2P and total RNAP. Surprisingly, Ser 5P was detected at the promoter and coding regions of many bivalent genes tested (8 out of 9 genes tested), but was absent from silent genes that lack bivalent chromatin (*Gata1*, *Myf5*, *λ5*) and have been shown to be unresponsive to withdrawal of PRC1 and 2 (refs 4, 7). Binding of Ser 5P to the promoters of bivalent genes was confirmed in three independent ES cell lines, but was not seen in trophoblast stem (TS) cells (see Supplementary Information, Fig. S1a), a closely related stem cell population with a far more restricted developmental potential. In TS cells, *Cdx2*, *Flk1* and *Gata4* promoters bound RNAP (detected by 8WG16; data not shown), consistent with expression of these genes in trophoblast tissues. In ES cells, binding of Ser 2P, a form of RNAP associated with elongation and recruitment of the RNA processing machinery², was not enriched at any of the bivalent genes analysed but instead, was detected within the coding (or promoter) regions of expressed *β-actin*, *Oct4* and *Sox2* genes (Fig. 1a). Collectively, these results show that RNAP is present at bivalent genes in pluripotent ES cells and is preferentially phosphorylated at Ser 5, but not at Ser 2.

The specificity of antibodies for total RNAP, Ser 2P and Ser 5P has been extensively characterized previously¹⁷, but was confirmed using ES cell extracts prepared in the presence of phosphatase inhibitors and

¹Nuclear Organisation, ²Lymphocyte Development and ³Developmental Epigenetics Groups, MRC Clinical Sciences Centre, Imperial College School of Medicine, Hammersmith Hospital Campus, Du Cane Road, London W12 0NN, UK. ⁴Department of Developmental and Cell Biology, Centro de Investigaciones Biológicas, CSIC, Madrid, Spain. ⁵Department of Developmental Genetics, RIKEN Research Center for Allergy and Immunology, RIKEN Yokohama Institute, Yokohama, Japan.

*Correspondence should be addressed to: A.P. or A.G.F. (e-mail: ana.pombo@csc.mrc.ac.uk; amanda.fisher@csc.mrc.ac.uk)

*These authors contributed equally to this work.

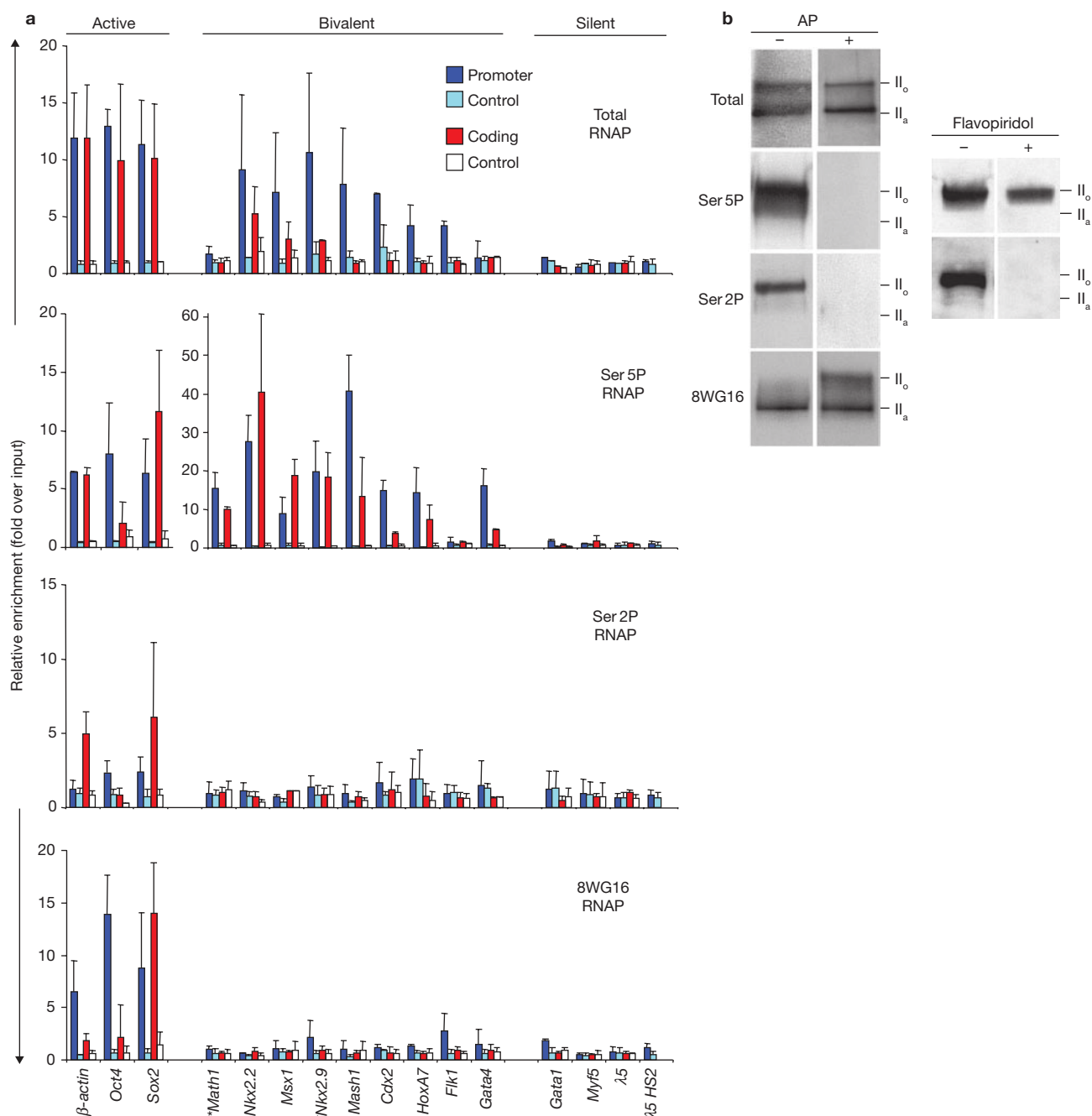


Figure 1 Poised RNAP phosphorylated on Ser 5 marks bivalent genes in ES cells. **(a)** Abundance of different phosphorylated forms of RNAPII at active, bivalent and silent genes in murine ES-OS25 cells assessed by ChIP and qPCR at promoter (blue bars) and coding regions (red bars). Bivalent genes important for subsequent neural specification (*Math1*, *Nkx2.2*, *Msx1*, *Nkx2.9* and *Mash1*), or for extra-embryonic (*Cdx2*), mesodermal (*HoxA7*, *Flk1*) and endodermal (*Gata4*) differentiation are shown. Promoter primers are positioned within -400 base pairs (bp) of transcription start sites, except for *Sox2* (-670 bp). Coding region primers are positioned $+2$ to $+4$ kb from start sites, except for *Sox2* ($+617$ bp). Additional sites in the coding region of several genes consistently showed the presence of RNAP (8 sites in *Nkx2.2* and *Gata4*, 4 in *Msx1*, 3 in *Cdx2*, and 2 in *Mash1* and *Flk1*). * indicates small genes of <2 kb. Enrichment is expressed relative to input DNA using the same amount of DNA in the PCR. Background levels (mean enrichment from control antibodies and beads alone) at promoter and coding regions are shown as pale blue or white bars, respectively. Mean and standard deviations

are presented from 3–5 independent experiments, except for total RNAP (two independent experiments). **(b)** Reactivity of different RNAP antibodies against hyper- (II_o) and hypophosphorylated (II_a) forms of the largest subunit of RNAP, RPB1, was assessed by western blotting using whole-cell extracts from ES-OS25 cells treated $\pm 10 \mu\text{M}$ flavopiridol. SDS-PAGE resolves RPB1 into II_o and II_a forms (also see Supplementary Information, Fig. S7a). Both forms are detected by an antibody against the amino-terminus (H224) that binds independently of phosphorylation. An antibody against the Ser 5P CTD peptide (4H8) recognizes the II_o and intermediately phosphorylated bands and has low sensitivity to flavopiridol. Ser 2P RNAP is recognized by H5, which detects only the II_o band and is highly sensitive to flavopiridol. Both 4H8 and H5 reactivities are dependent on phosphorylated epitopes, as shown by treatment of western blot membranes with alkaline phosphatase (AP). An antibody against unphosphorylated CTD (8WG16) detects II_a and intermediately phosphorylated bands, but not highly phosphorylated II_o; AP treatment allows reactivity with II_o.

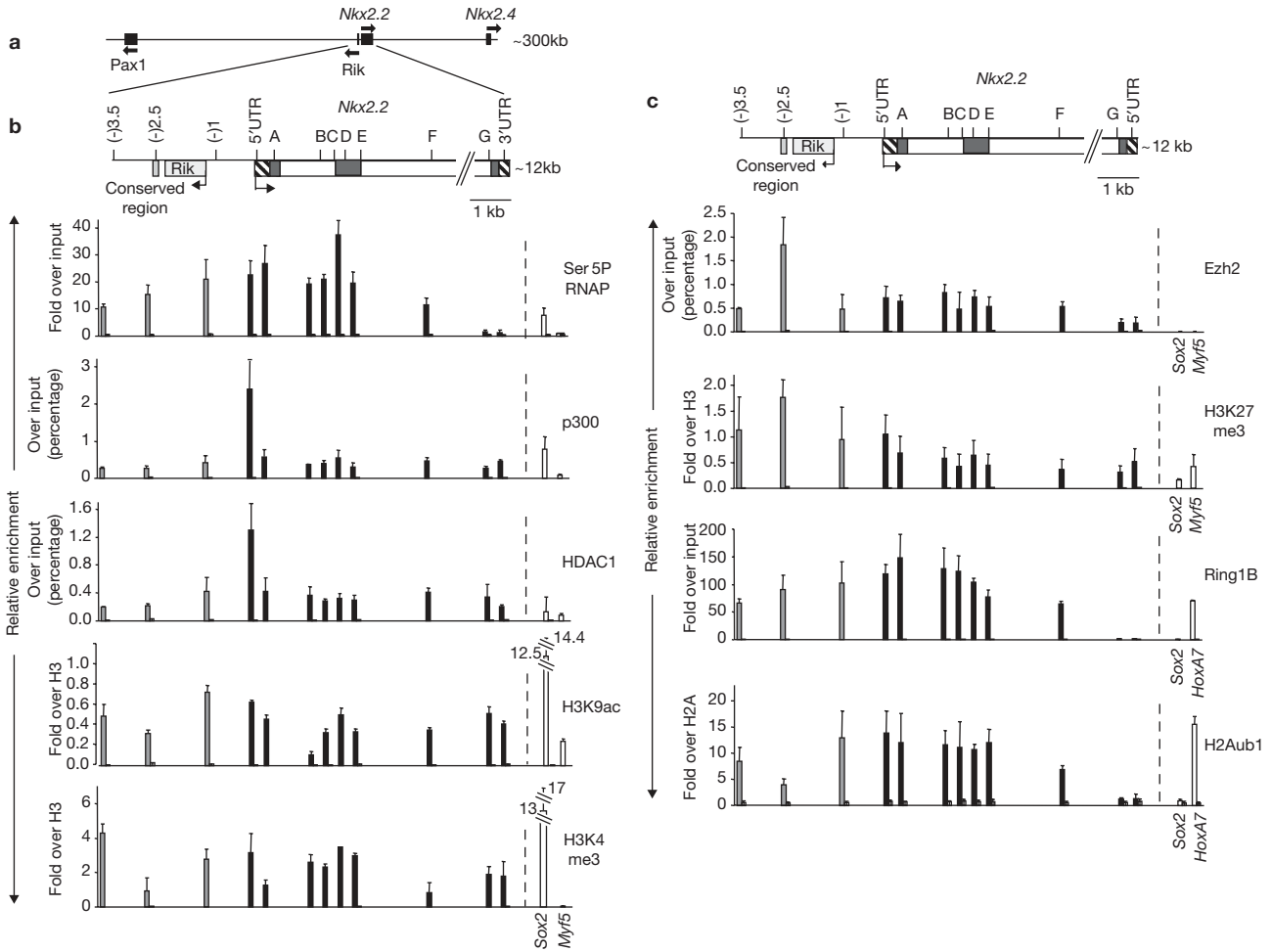


Figure 2 Mapping the binding of transcription machinery and Polycomb repressor components at bivalent chromatin domains in the *Nkx2.2* locus in ES cells. **(a)** Diagram illustrating the genomic context of *Nkx2.2* on mouse chromosome 2. *Nkx2.2* is within a gene-poor region (Ensembl v37, Feb 2006) but is flanked by three genes, *Nkx2.4*, *Pax1* and a gene of unknown function (*Rik*; 6430503K07*Rik*), all of which are silent in ES cells. Arrows indicate direction of transcription. **(b)** ChIP analysis of a 12 kb region of *Nkx2.2* that spans -3.5 kb (upstream of transcription start site; arrow), a conserved region at -2.5 kb (light grey box), and the entire coding region of 8.7 kb containing three exons (dark grey boxes) and untranslated regions (striped boxes). The position of primer pairs used for ChIP analyses is indicated by name or letter. Ser 5P RNAP, p300, HDAC1, H3K9ac and H3K4me3 occupancy across the *Nkx2.2* gene locus was assessed in ES-OS25 cells using ChIP and qPCR. **(c)** Binding of PRC2 and PRC1

components, Ezh2 and Ring1B, and associated histone modifications, H3K27me3 and H2Aub1, across the *Nkx2.2* gene locus. **(b,c)** Enrichment is shown relative to input DNA using the same amount of DNA in the PCR (for Ser 5P, Ring1B, H2Aub1), or relative to total input DNA (for p300, HDAC1, H3K9ac, H3K4me3, H3K27me3, Ezh2), according to the ChIP protocol used to optimize detection. Histone modifications are normalized to unmodified core histones (H3 or H2A). Active (*Sox2*) and silent (*Myf5*) genes were used as controls. *HoxA7*, a known PRC1 target, was used as a positive control for Ring1B and H2Aub1. Background levels, mean enrichment from control antibodies and beads alone (for Ser 5P, Ring1B, H2Aub1), or enrichment from control antibody (for p300, HDAC1, H3K9ac, H3K4me3, Ezh2, H3K27me3) are presented (black bars) next to each data point, and were generally low or negligible. Mean and standard deviations are presented from three independent experiments.

separated by SDS-PAGE to resolve hypo- (II_a) and hyperphosphorylated (II_o) RNAP forms (Fig. 1b). As shown, 4H8 (Ser 5P) and H5 (Ser 2P) antibodies detected II_o and this reactivity was abolished by pre-treatment of transferred proteins with alkaline phosphatase. H224 (used for total RNAP) detects II_a and II_o similarly, whereas antibody 8WG16, a reagent used previously for genome-wide ChIP studies^{8,11}, recognises predominantly II_a and some intermediately phosphorylated forms¹⁷. In our ChIP assay, RNAP at bivalent genes was weakly detected by 8WG16 (Fig. 1a). Binding of 8WG16 to the II_o form was demonstrated in western blots following dephosphorylation of the transferred proteins, consistent with phosphorylation obscuring 8WG16 binding (Fig. 1b). The specificity of H5 and 4H8 for Ser 2P and Ser 5P, respectively, was validated using

flavopiridol, a potent inhibitor of CDK9, an enzyme that phosphorylates Ser 2 residues, but a weak inhibitor of CDK7, which targets Ser 5 (ref. 18). As predicted, 4H8 detected phosphorylated forms that were unaffected by flavopiridol treatment (Ser 5P), whereas H5 recognition of Ser 2P was abolished (Fig. 1b; see Supplementary Information, Fig. S1b).

To investigate the distribution of Ser 5P at bivalent loci relative to other transcriptional components and chromatin markers, we used ChIP approaches to examine sites spanning the entire *Nkx2.2* locus on chromosome 2 (Fig. 2). *Nkx2.2* is normally expressed by ventral progenitors of the central nervous system in response to high levels of Shh-Gli signalling^{19,20}, is silent in ES cells, and was previously shown to be up-regulated in ES cells deficient in H3K27 methylation⁴. Ser 5P was detected

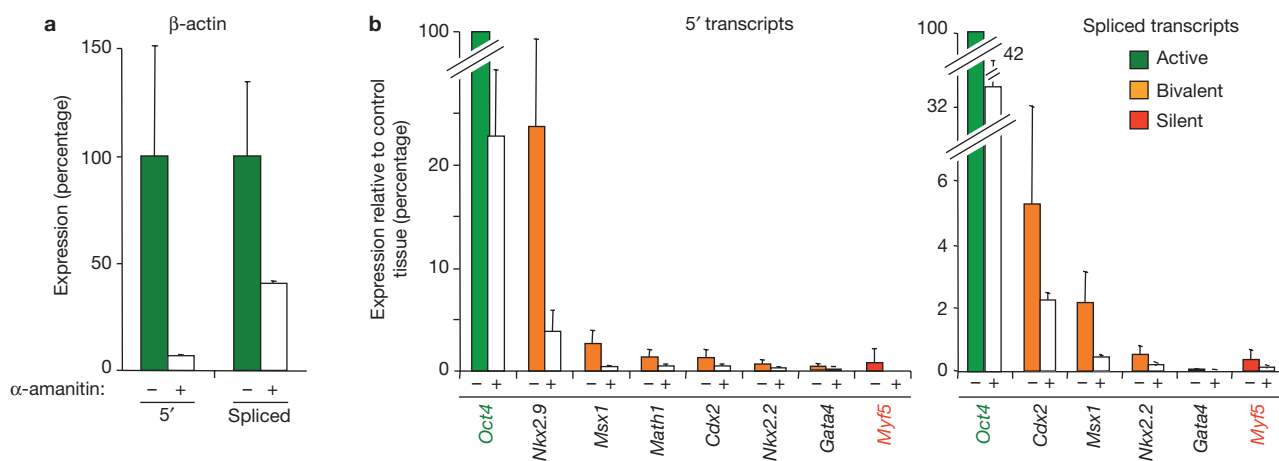


Figure 3 Bivalent genes are transcribed at low level in ES cells. RNA levels were measured by quantitative RT-PCR using ES cells incubated in the absence or presence of α -amanitin ($75 \mu\text{g ml}^{-1}$ for 7 h, to block RNAPII transcription; negative control, open bars). 5' primers amplifying transcripts spanning the exon 1 and intron 1 junction were used to detect primary transcripts and spliced transcripts were detected using primers located at the exon 1 and exon 2 junction. (a) As shown for β -actin, treatment with α -amanitin reduced primary transcripts by 93% and spliced transcripts by 60%, consistent with a stable pool of β -actin mRNA in ES cells. (b) Transcripts

derived from genes that are active (green), silent (red) and bivalent (orange) in ES cells were detected using appropriately positioned primers to assess primary and spliced transcripts. Low levels of 5' and spliced transcripts were detected for all bivalent genes tested, and these were sensitive to inhibition by α -amanitin. These findings indicate that RNAP initiates and elongates at bivalent genes. The results obtained from three independent experiments were normalized to house-keeping genes and values expressed relative to control tissues: embryonic (E15) head (for *Nkx2.9*, *Math1*, *Nkx2.2*, *Msx1*), adult heart (*Gata4*), TS cells (*Cdx2*), C2C12 cells (*Myf5*) and ES-OS25 cells (*Oct4*).

upstream (0–3.5 kb) of the coding region of *Nkx2.2* and within the gene (peak enrichment in the first and second exons), but little binding was detected at downstream regions (exon 3 and 3'UTR, 8 kb from the promoter; Fig. 2b; see Supplementary Information Fig. S1c for an accurate estimate for the resolution of the ChIP approach used here). Interestingly, HDAC1 and p300, two other components of the transcription machinery, also bound at the silent *Nkx2.2* locus in ES cells, with a prominent peak in the 5'UTR. Co-binding of HDAC1 and p300 at promoters of many other bivalent genes was also observed (data not shown). Conventional markers of active euchromatin, including histone H3K9ac and H3K4me3, were enriched throughout *Nkx2.2*, with prominent peaks at -3.5 kb, at the promoter region (-1 to 5'UTR) and within exon 2 (Fig. 2b). The abundance of Ser 5P, p300, HDAC1 and active chromatin marks detected within upstream regions (-3.5 to -1 kb; Fig. 2b) could reflect priming of a RIKEN gene of unknown function that is not expressed in ES cells (data not shown). Histone H3K27me3 and Ezh2, the HMTase responsible for the catalytic activity of PRC2 (refs 21,22), were present throughout *Nkx2.2*, being particularly enriched in the upstream (-2.5 kb) domain (Fig. 2c). Ring1B, a component of PRC1 that catalyses mono-ubiquitination of histone H2A at lysine 119 (H2Aub1)^{23,24}, was enriched throughout the locus and binding peaked at the first and second exons, similarly to RNAP (Fig. 2c). Consistent with these findings, ChIP analysis for H2Aub1 showed enrichment of this modified histone in the upstream and 5' coding regions of the *Nkx2.2* gene.

The specificity of H2Aub1 ChIP was verified using control genes that are targets for PRC1-mediated modification in ES cells (*HoxA7*; ref. 25) or that are not targets (*Sox2*; Fig. 2c), and using Ring1B-deficient ES cells (see Supplementary Information, Fig. S2a and below). As expected, Ring1B and H2Aub1 were found at all bivalent genes tested⁶ (see Supplementary Information, Fig. S2b). These data show that Ser 5P, HDAC1 and p300 co-locate with PRC1- and PRC2-components at the promoter region of the *Nkx2.2* gene when it is silent in ES cells. Ser 5P is

seen to extend into the 5' coding regions of *Nkx2.2* (exons 1 and 2) where active (H3K9ac, H3K4me3) and repressive (H3K27me3, H2Aub1) histone modifications are also abundant. To confirm that these characteristics are shared by other 'bivalent' loci in ES cells, ChIP analysis was also used to profile the *Msx1* locus on chromosome 5 (see Supplementary Information, Fig. S3). As observed for *Nkx2.2*, high levels of Ser 5P decorate the 5' regulatory regions of *Msx1* and extend into the coding region of the gene (up to 3 kb). Binding of the transcriptional machinery and distribution of histone modifications were also similar to that previously shown for *Nkx2.2* (see Supplementary Information, Fig. S3).

To directly assess whether RNAP that is present at bivalent genes is transcriptionally active, the production of 5' and spliced transcripts in ES cells was measured using RT-PCR (Fig. 3). Relative to productively expressed genes such as β -actin and *Oct4*, low levels of 5' and spliced transcripts corresponding to many bivalent genes (*Nkx2.9*, *Gata4*, *Msx1*, *Math1*, *Cdx2*, *Nkx2.2*) were detected in ES cells and were sensitive to the RNAP inhibitor α -amanitin (Fig. 3b). Consistent with recent observations in human cells¹², these results confirm that many bivalent loci are transcribed at low levels in mouse ES cells. Although RNAP levels are comparable to productively expressed genes, the low levels of 5' transcripts detected suggests either that elongation is inefficient at bivalent genes, or that transcripts are rapidly degraded. This situation contrasts with overt transcription, where RNAP assumes a configuration that is typical of expressed genes. For example, *Gata4*, a gene that is bivalent in ES cells but abundantly expressed in testes, heart and primitive endoderm, showed high levels of Ser 2P (throughout the coding region) and 8WG16 binding (at the promoter) in XEN cells derived from the primitive endoderm (see Supplementary Information, Fig. S4).

Previous studies have demonstrated that bivalent genes are de-repressed in ES cell lines homozygous for a null mutation in the PRC2 Polycomb repressor protein Eed^{4,6,7}. The PRC1 complex is thought to function downstream of PRC2 (refs 21, 22, 26), and recent studies

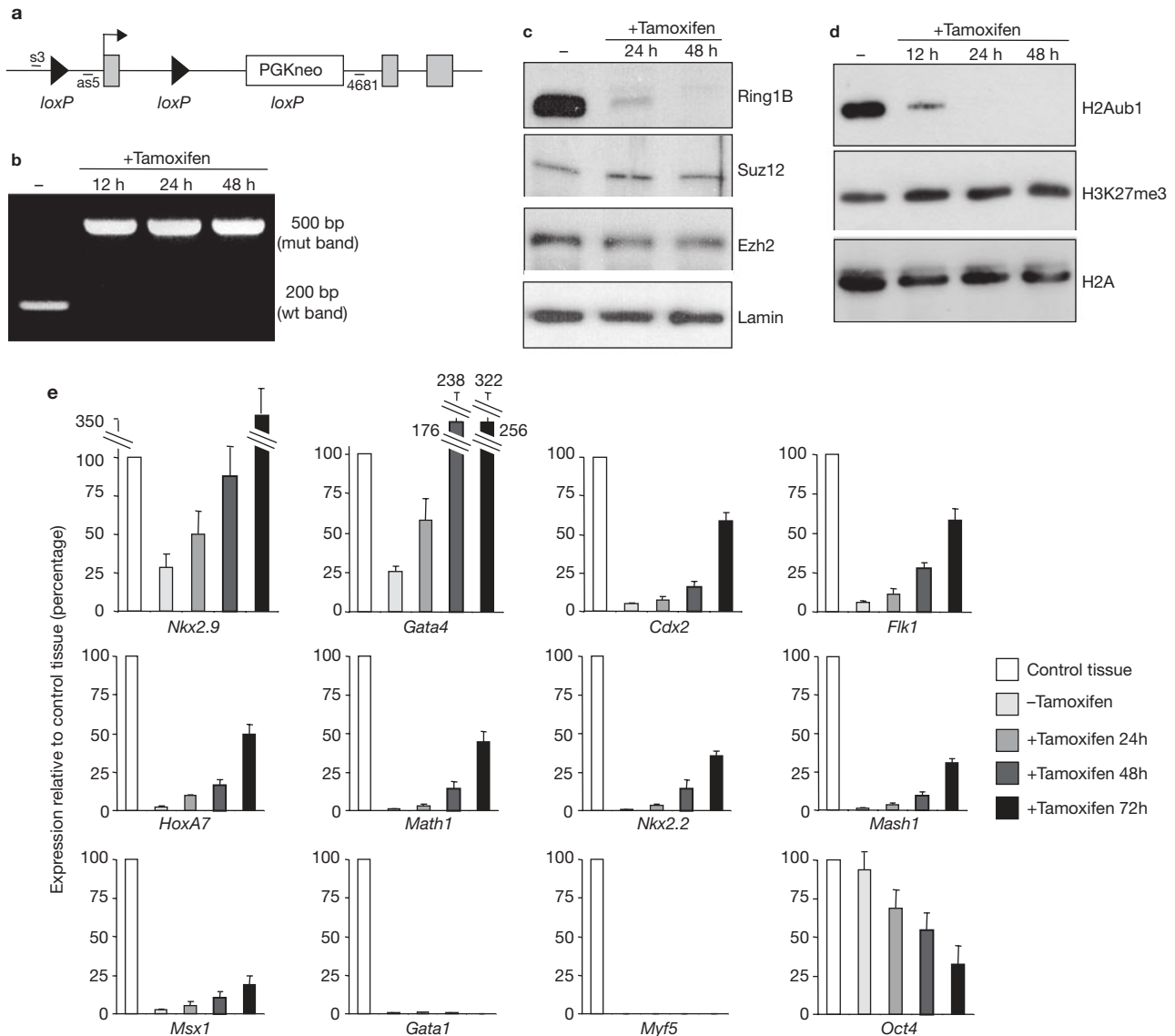


Figure 4 Conditional removal of Ring1B results in a rapid decline in global levels of mono-ubiquitinated H2A and selective de-repression of bivalent genes in ES cells. **(a)** Schematic representation of the *Ring1B* conditional allele. s3, as5 and 4681 are the annealing sites for primers used to check efficient deletion of the *Ring1B* gene in ES-Ert2 cells. **(b)** ES-Ert2 cells containing the *Ring1B* conditional allele were cultured in the presence of 800 nM tamoxifen for 0–48 h. Genomic DNA was extracted and analysed by PCR for the presence of wild-type (wt) and deleted (mut) *Ring1B* alleles. **(c)** Western blot analysis of nuclear extracts of ES-Ert2 cells cultured with 800 nM tamoxifen for 0–48 h, using anti-Ring1B, anti-Suz12, anti-Ezh2, and anti-Lamin (loading control) antibodies. Full-length blot scans

are presented in Supplementary Information, Fig. S7b. **(d)** Western blot of acid-extracted histones from ES-Ert2 cells cultured with 800 nM tamoxifen for 0–48 h, using anti-H2Aub1, anti-H3K27me3 and anti-H2A (loading control) antibodies. Full-length blot scans are presented in Supplementary Information, Fig. S7c. **(e)** Kinetics of gene expression in ES-Ert2 cells following tamoxifen treatment. Gene expression was assessed by quantitative RT-PCR. Mean and standard deviation from more than three experiments are represented relative to housekeeping genes and expressed relative to control tissues: embryonic (E15) heads (*Nkx2.9*, *Math1*, *Nkx2.2*, *Mash1*, *Msx1*), embryonic liver (*Gata4*), TS cells (*Cdx2*), spleen (*Flk1*, *HoxA7*, *Gata1*), C2C12 cells (*Myf5*) and ES-OS25 (*Oct4*).

suggest that it mediates repression by functioning as a ubiquitin E3 ligase specific for histone H2A lysine 119 (refs 23, 24). To understand the role of Polycomb repressors in maintaining RNAP in a poised configuration, we used ES-Ert2, an ES cell line, that carries a tamoxifen-inducible, conditional knockout of the core PRC1 protein Ring1B, and is also homozygous null for the functional homologue Ring1A. Thus, following addition of tamoxifen, ES-Ert2 cells are progressively depleted of Ring1B protein and global H2A ubiquitination, whereas overall levels of PRC2 proteins and associated H3K27me3 are largely unaffected

(Fig. 4a–d). Microarray expression analysis of ES-Ert2 cells following Ring1B deletion has demonstrated rapid de-repression of Polycomb target genes which, in turn, triggers widespread differentiation of ES-Ert2 cells approximately 3–4 days after addition of tamoxifen (M.V. and H.K., data not shown). Consistent with these findings, we observed de-repression of bivalent genes within 72 h of treatment (Fig. 4e). Notably, genes such as *Gata4*, *Nkx2.9* and *HoxA7* were markedly de-repressed within 48 h following addition of tamoxifen. In contrast, repression of the non-bivalent genes *Gata1* and *Myf5* was unaffected.

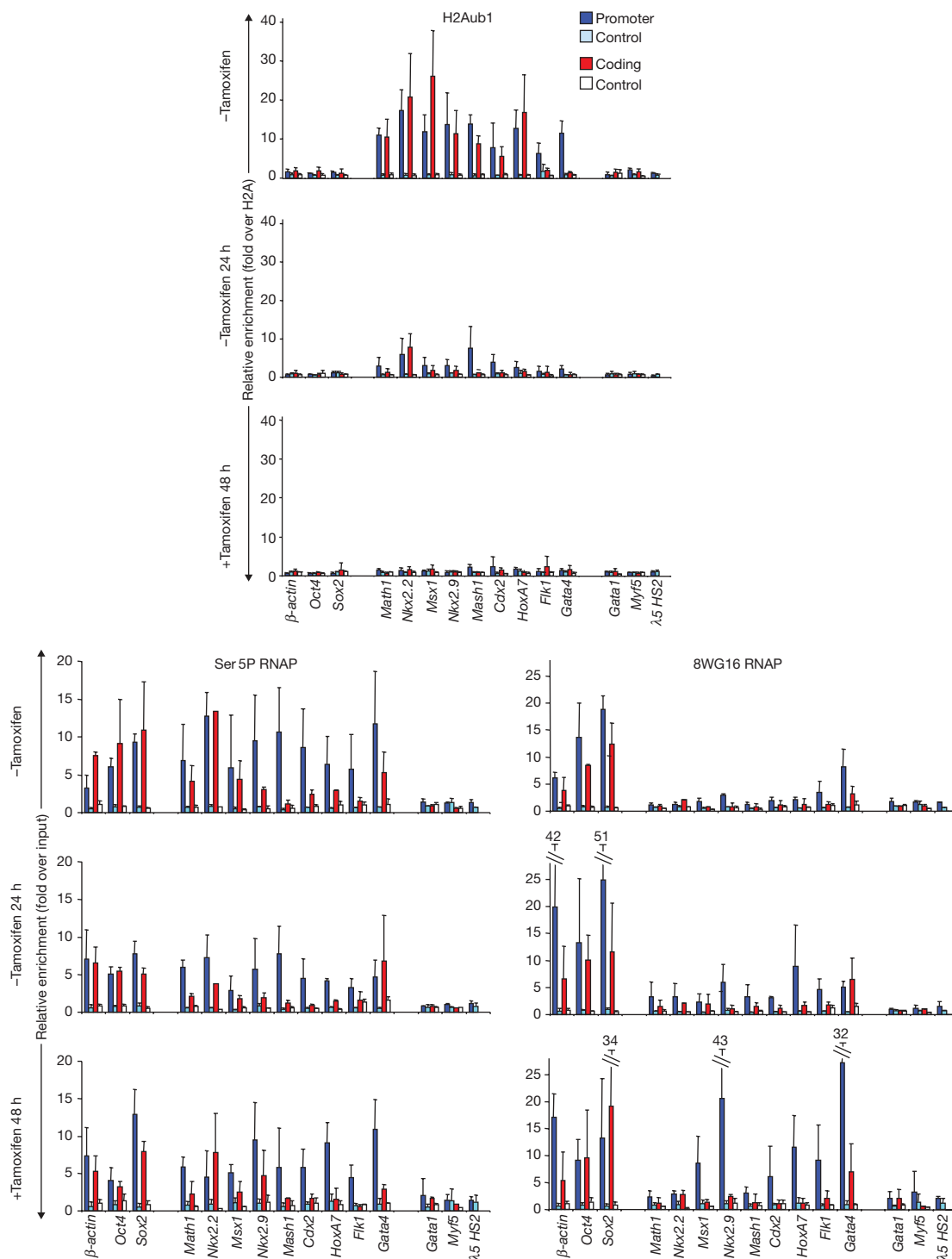


Figure 5 Loss of H2Aub1 results in changes in RNAP conformation at bivalent genes in ES cells. The abundance of H2Aub1, Ser 5P and 8WG16 RNAP was assessed at the promoter (blue bars) and coding regions (red bars) of bivalent genes after 0, 24 and 48 h tamoxifen treatment of ES-ERT2 cells to excise the *Ring1B* gene. Enrichment is expressed relative to input DNA using the same amount of DNA in the PCR and H2Aub1 is normalized

to H2A. Background levels (mean enrichment from control antibodies and beads alone) at promoter and coding regions are shown as pale blue or white bars, respectively. Mean and standard deviations are presented from 3–4 independent ChIP experiments. Differences in abundance of H2Aub1, Ser 5P and 8WG16 RNAP at bivalent genes with time were statistically significant ($P < 0.0001$, $P = 0.02$ and $P = 0.002$, respectively; ANOVA).

Based on these observations, we examined early events occurring at bivalent gene promoters within the first 48 h following tamoxifen treatment and deletion of *Ring1B*. At this time ES-ERT2 cells remain

undifferentiated, as validated by the continued expression of proteins such as Oct4, Nanog, Rex1, SSEA-1 and alkaline phosphatase (see Supplementary Information, Fig. S5). ChIP analysis demonstrated

a modest decrease in levels of the PRC2 protein Ezh2 and associated H3K27me3 by 48 h, but no statistically significant change in the levels of H3K4me3 (see Supplementary Information, Fig. S6a–c). On the other hand, levels of Ring1B and H2Aub1 at bivalent genes fell markedly, and were essentially undetectable after 48 h (see Supplementary Information, Fig. S6d and Fig. 5, respectively). During this time period changes in RNAP were analysed. Levels of the Ser 5P form of RNAP remained high at bivalent genes (Fig. 5), and Ser 2P levels were unchanged (see Supplementary Information, Fig. S6e). However, RNAP levels detected with 8WG16, which were initially very low at bivalent genes in ES cells, increased markedly within 24 h following deletion of *Ring1B*, and increased further after 48 h (Fig. 5). The increased levels of 8WG16 RNAP correlate well with the rate at which specific bivalent genes undergo de-repression. As expected, 8WG16 RNAP and expression levels at silent non-bivalent genes were unaffected by *Ring1B* deletion.

Collectively, the data presented here suggest that at bivalent genes where Ser 5P predominates in ES cells, RNAP may have an unusual conformation that is not detected efficiently by 8WG16. This conformation is clearly different from the paused RNAP previously described in differentiated cells, as Ser 5P levels are generally higher in bivalent genes and extend into coding regions (Figs 1a, 2, S3, S4). RNAP at bivalent genes is associated with the production of low levels of α -amanitin-sensitive transcripts in ES cells (Fig. 3) and with a lack of Ser 2P (Fig. 1a), a modification that may influence the overall yield of mature transcripts². We have provided evidence that RNAP present at silent bivalent genes in ES cells is held in check by PRC1-mediated mono-ubiquitination of H2A. Removal of the PRC1 catalytic Ring1A- and B-components results in changes in the RNAP complexes, and subsequently, in productive gene expression (Fig. 4e, 5), demonstrating a key role for PRC1 in maintaining the poised RNAP conformation in wild-type ES cells. Although the failure of previous ChIP-on-Chip studies to detect abundant RNAP at bivalent genes may reflect the lower sensitivity of whole genome assays, our data give evidence of an unusual or poised configuration of RNAP in ES cells. A recent study by Guenther *et al.*¹² has described the presence of H3K4me3 at the promoters of most genes in human ES cells and has also detected the presence of RNAP at bivalent genes and their respective transcripts. Chromatin profiling of human ES cells has also suggested that H3K4me3 mark more genes than was previously recognised and that these 'bivalent' domains may not be restricted to ES cells³⁰. We have demonstrated that changes in RNAP conformation following *Ring1B* deletion, highlighted by an increase in 8WG16 binding, occur without major changes in Ser 5 or Ser 2 phosphorylation (Fig. 5, S6e). This suggests that gene de-repression is not due to increases either in initiation efficiency, or in the formation of a typical elongation complex. Instead, the rapid shift in RNAP conformation implies that Ring1-mediated H2A ubiquitination has a direct role in limiting RNAP processivity at bivalent genes. This interpretation is consistent with TBP and HDAC1 loading at Polycomb target genes in *Drosophila melanogaster*²⁷, and with the observation that Polycomb repression does not interfere with RNAP recruitment at the *hsp26* promoter, but instead influences downstream events in the transcription cycle²⁸. In the context of ES cells, where Polycomb proteins repress an important cohort of developmental regulators required to execute alternative lineage paths, the observation that RNAP is recruited to bivalent genes and restrained by Ring1 and H2Aub1, provides a crucial conceptual advance in our understanding of how stem cell pluripotency is achieved. □

METHODS

A detailed description of materials and methods is given in Supplementary Information.

Chromatin immunoprecipitation. ChIP assays were performed as described previously^{4,29}, except for some modifications introduced for increased efficiency using RNAP and H2Aub1 antibodies. Experimental details, including antibodies used, can be found in Supplementary Information.

Western blot analysis. Standard procedures were used for western blotting, except that phosphatase inhibitors were used. See Supplementary Information for antibodies used and experimental details.

RNA purification and RT-PCR analysis. RT-PCR was performed as described previously⁴. See Supplementary Information, Table 2, for primer sequences.

FACS analysis, immunofluorescence and alkaline phosphatase activity assay. Fixed cells were stained for Nanog, SSEA-1 or Oct4 proteins and analysed on a FACScalibur or by immunofluorescence. Alkaline phosphatase activity assays were performed according to the manufacturer's instructions (Sigma). See Supplementary Information for experimental details.

Note: Supplementary Information is available on the Nature Cell Biology website.

ACKNOWLEDGEMENTS

We thank Henrietta Szutorisz, Niall Dillon, Miguel R. Branco (CSC) and Stephen Buratowski (Harvard Medical School, Cambridge, MA) for advice establishing the RNAP ChIP, James Briscoe (MRC-NIMR) and Joana Santos (CSC) for help in the design of *Nkx2.2* gene analyses and TS cell culture, Austin Smith (Wellcome Trust Centre for Stem Cell Research, Cambridge, UK) for ES-OS25 and ES-ZHBTc4 cells, Janet Rossant (Hospital for Sick Children, Toronto, Canada) for XEN cells, Sanofi-Aventis (Bethesda, MD) for the kind gift of flavopiridol, Francisco Ramirez (London, UK) for the statistical analyses, Zoe Webster (CSC) for assistance with ES cell culture, Matthias Merckenschlager and Sarah Elderkin (CSC) for advice and the Medical Research Council (UK), Genome Network Project and NoE Epigenome for support.

AUTHOR CONTRIBUTIONS

M.C. and E.B. contributed equally to this work.

Published online at <http://www.nature.com/naturecellbiology/>

Reprints and permissions information is available online at <http://npg.nature.com/reprintsandpermissions/>

- Buratowski, S. The CTD code. *Nature Struct. Biol.* **10**, 679–680 (2003).
- Phatnani, H. P. & Greenleaf, A. L. Phosphorylation and functions of the RNA polymerase II CTD. *Genes Dev.* **20**, 2922–2936 (2006).
- Saunders, A., Core, L. J. & Lis, J. T. Breaking the barriers to transcription elongation. *Nature Rev. Mol. Cell Biol.* **7**, 557–567 (2006).
- Azuara, V. *et al.* Chromatin signatures of pluripotent cell lines. *Nature Cell Biol.* **8**, 532–538 (2006).
- Bernstein, B. E. *et al.* A bivalent chromatin structure marks key developmental genes in embryonic stem cells. *Cell* **125**, 315–326 (2006).
- Boyer, L. A. *et al.* Polycomb complexes repress developmental regulators in murine embryonic stem cells. *Nature* **441**, 349–353 (2006).
- Jørgensen, H. F. *et al.* Stem cells primed for action: polycomb repressive complexes restrain the expression of lineage-specific regulators in embryonic stem cells. *Cell Cycle* **5**, 1411–1414 (2006).
- Lee, T. I. *et al.* Control of developmental regulators by Polycomb in human embryonic stem cells. *Cell* **125**, 301–313 (2006).
- Spivakov, M. & Fisher, A. G. Epigenetic signatures of stem-cell identity. *Nature Rev. Genet.* **8**, 263–271 (2007).
- Bracken, A. P. *et al.* The Polycomb group proteins bind throughout the INK4A-ARF locus and are dissociated in senescent cells. *Genes Dev.* **21**, 525–530 (2007).
- Squazzo, S. L. *et al.* Suz12 binds to silenced regions of the genome in a cell-type-specific manner. *Genome Res.* **16**, 890–900 (2006).
- Guenther, M. G., Levine, S. S., Boyer, L. A., Jaenisch, R. & Young, R. A. A chromatin landmark and transcription initiation at most promoters in human cells. *Cell* **13**, 77–88 (2007).
- Maniatis, T. & Reed, R. An extensive network of coupling among gene expression machines. *Nature* **416**, 499–506 (2002).
- Boehm, A. K., Saunders, A., Werner, J. & Lis, J. T. Transcription factor and polymerase recruitment, modification, and movement on *dhsp70* in vivo in the minutes following heat shock. *Mol. Cell. Biol.* **23**, 7628–7637 (2003).

15. Espinosa, J. M., Verdun, R. E. & Emerson, B. M. p53 functions through stress- and promoter-specific recruitment of transcription initiation components before and after DNA damage. *Mol. Cell* **12**, 1015–1027 (2003).
16. Spilianakis, C. *et al.* CIITA regulates transcription onset via Ser 5-phosphorylation of RNA Pol II. *EMBO J.* **22**, 5125–5136 (2003).
17. Xie, S. Q., Martin, S., Guillot, P. V., Bentley, D. L. & Pombo, A. Splicing speckles are not reservoirs of RNA polymerase II, but contain an inactive form, phosphorylated on serine 2 residues of the C-terminal domain. *Mol. Biol. Cell* **17**, 1723–1733 (2006).
18. Chao, S. H. & Price, D. H. Flavopiridol inactivates P-TEFb and blocks most RNA polymerase II transcription *in vivo*. *J. Biol. Chem.* **276**, 31793–31799 (2001).
19. Ericson, J. *et al.* Pax6 controls progenitor cell identity and neuronal fate in response to graded Shh signaling. *Cell* **90**, 169–180 (1997).
20. Stamatakis, D., Ulloa, F., Tsoni, S. V., Mynett, A. & Briscoe, J. A gradient of Gli activity mediates graded Sonic Hedgehog signaling in the neural tube. *Genes Dev.* **19**, 626–641 (2005).
21. Cao, R. *et al.* Role of histone H3 lysine 27 methylation in Polycomb-group silencing. *Science* **298**, 1039–1043 (2002).
22. Kuzmichev, A., Nishioka, K., Erdjument-Bromage, H., Tempst, P. & Reinberg, D. Histone methyltransferase activity associated with a human multiprotein complex containing the Enhancer of Zeste protein. *Genes Dev.* **16**, 2893–2905 (2002).
23. de Napoles, M. *et al.* Polycomb group proteins Ring1A/B link ubiquitylation of histone H2A to heritable gene silencing and X inactivation. *Dev. Cell* **7**, 663–676 (2004).
24. Wang, H. *et al.* Role of histone H2A ubiquitination in Polycomb silencing. *Nature* **431**, 873–878 (2004).
25. Cao, R., Tsukada, Y. & Zhang, Y. Role of Bmi-1 and Ring1A in H2A ubiquitylation and Hox gene silencing. *Mol. Cell* **20**, 845–854 (2005).
26. Hernandez-Munoz, I., Taghavi, P., Kuijl, C., Neefjes, J. & van Lohuizen, M. Association of BMI1 with polycomb bodies is dynamic and requires PRC2/EZH2 and the maintenance DNA methyltransferase DNMT1. *Mol. Cell. Biol.* **25**, 11047–11058 (2005).
27. Breiling, A., Turner, B. M., Bianchi, M. E. & Orlando, V. General transcription factors bind promoters repressed by Polycomb group proteins. *Nature* **412**, 651–655 (2001).
28. Dellino, G. I. *et al.* Polycomb silencing blocks transcription initiation. *Mol. Cell* **13**, 887–893 (2004).
29. Szutorisz, H. *et al.* Formation of an active tissue-specific chromatin domain initiated by epigenetic marking at the embryonic stem cell stage. *Mol. Cell. Biol.* **25**, 1804–1820 (2005).
30. Sharov, A.A. & Ko, M.S.H. Human ES cell profiling broadens the reach of bivalent domains. *Cell Stem Cell* **1**, 237–238, 2007

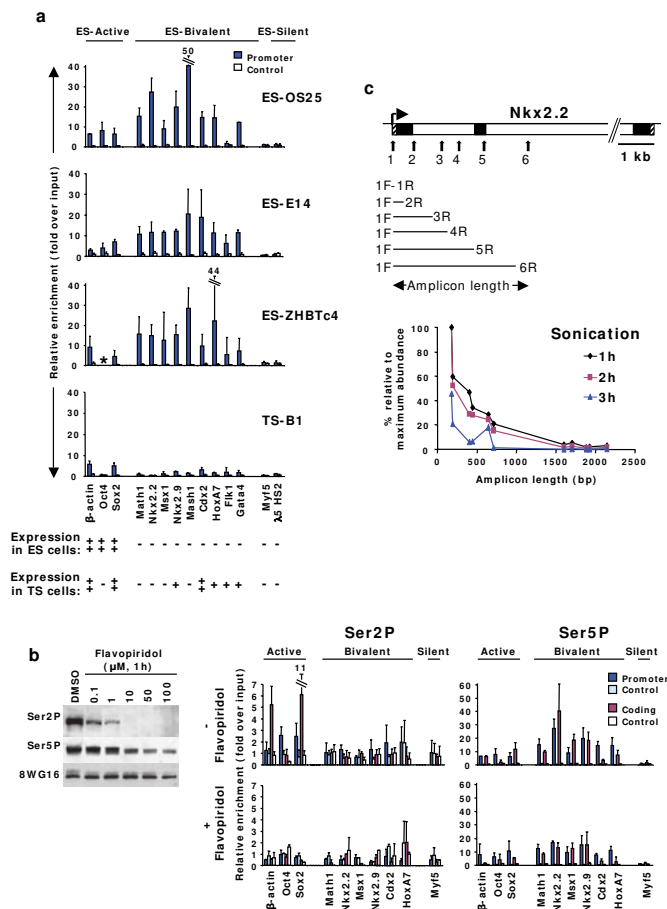


Figure S1 Ser5P RNAP binding in ES and TS cell lines; optimising the detection of Ser2P RNAP by ChIP; and resolution of ChIP assay used for detection of RNAP, Ring1B and H2Aub1. **(a)** Ser5P binding at the promoter of bivalent genes is a consistent feature of ES cell lines that is not seen in TS cells. The occupancy of Ser5P RNAP at the promoters (blue bars) of active, bivalent and silent genes was compared in ES-E14 cells and two derivative ES cell lines OS25 and ZHBTc4, using ChIP and qPCR. *Oct4* was not included in the ES-ZHBTc4 analysis as these cells contain an *Oct4* transgene (*). The occupancy of Ser5P RNAP within the promoter regions (blue bars) of these genes in TS-B1 cells is shown in the lower panel. Genes expressed in TS cells, such as *Cdx2*, showed some Ser5P enrichment. Enrichment is expressed relative to input DNA using the same amount of DNA in the PCR. Background levels (mean enrichment from control antibodies and beads alone) are shown as white bars. Mean and standard deviations are presented from 2 independent experiments. Gene expression was assessed in ES and TS cells by RT-PCR. **(b)** Optimising the detection of Ser2P RNAP using IgM antibodies. Titration of the concentration of flavopiridol necessary to deplete Ser2P levels after 1h treatment of ES-OS25 cells. Whole cell extracts were prepared from cells treated with 0.1–100 μM flavopiridol in DMSO, separated by SDS-PAGE and analysed by western blotting using H5, 4H8 and 8WG16. Flavopiridol treatment abolishes all detectable Ser2P RNAP at 10 μM, whereas Ser5P is still detected at 100 μM, albeit with a reduced signal. The levels of RNAP detected by 8WG16 remain constant at 10 μM, and are slightly reduced at 100 μM. Abundance of Ser2P and Ser5P RNAP at the promoter (blue bars) and coding regions (red bars) of active, bivalent and silent genes was assessed in ES-OS25 cells treated ± flavopiridol (10 μM, 1h), using ChIP and qPCR. Ser2P enrichment at active genes is fully sensitive to flavopiridol treatment,

as expected^{11,12}. Ser5P enrichment is partially reduced by flavopiridol, consistent with some inhibition of CDK7, but remains higher at bivalent than active genes. Enrichment is expressed relative to input DNA using the same amount of DNA in the PCR. Background levels (mean enrichment from control antibodies and beads alone) at promoter and coding regions are shown as pale blue or white bars, respectively. Mean and standard deviations are presented from 2 independent experiments. **(c)** Resolution of ChIP assay used for detection of RNAP, Ring1B and H2Aub1. ES cell chromatin was prepared as described in Supplementary Methods and sonicated for 1, 2 or 3h (30s 'on', 30s 'off'; 4°C). To obtain an accurate estimate of the resolution, qPCRs were run for amplicons of increasing size (179 to 2146 bp) across the *Nkx2.2* gene. To normalise for differences in PCR efficiency between products, PCRs were run in parallel using unsonicated BAC DNA containing the *Nkx2.2* gene (RP24-555M6, BACPAC Resources Centre). Primer positions are indicated on *Nkx2.2* gene diagram. Forward (F) primer #1 was run with #1, #2, #3, #4, #5 and #6 reverse (R) primers (indicated in the diagram), and #6 reverse (R) primer was run with #1, #2, #3, #4, #5 and #6 forward (F) primers. Quantitative PCR analysis of sonicated DNA. Sonicated DNA "cycle over threshold" (Ct) values (Son Ct) were subtracted from the BAC DNA Ct values (BAC Ct). This figure was converted into relative abundance by $2^{(BAC Ct - Son Ct)}$. The results for increasing amplicon size are represented in the graph as percentage of maximum abundance for the shortest amplicon (179 bp, 1h sonication). The resolution of ChIP after 1h sonication was <1600 bp; the percentage of amplified DNA decreases to <5% for amplicons sizes ≥1600 bp. Increasing sonication time to 2h does not significantly improve the resolution and after 3h the signal is reduced by 55% for the shortest amplicon, suggesting that longer sonication times may result in DNA degradation.

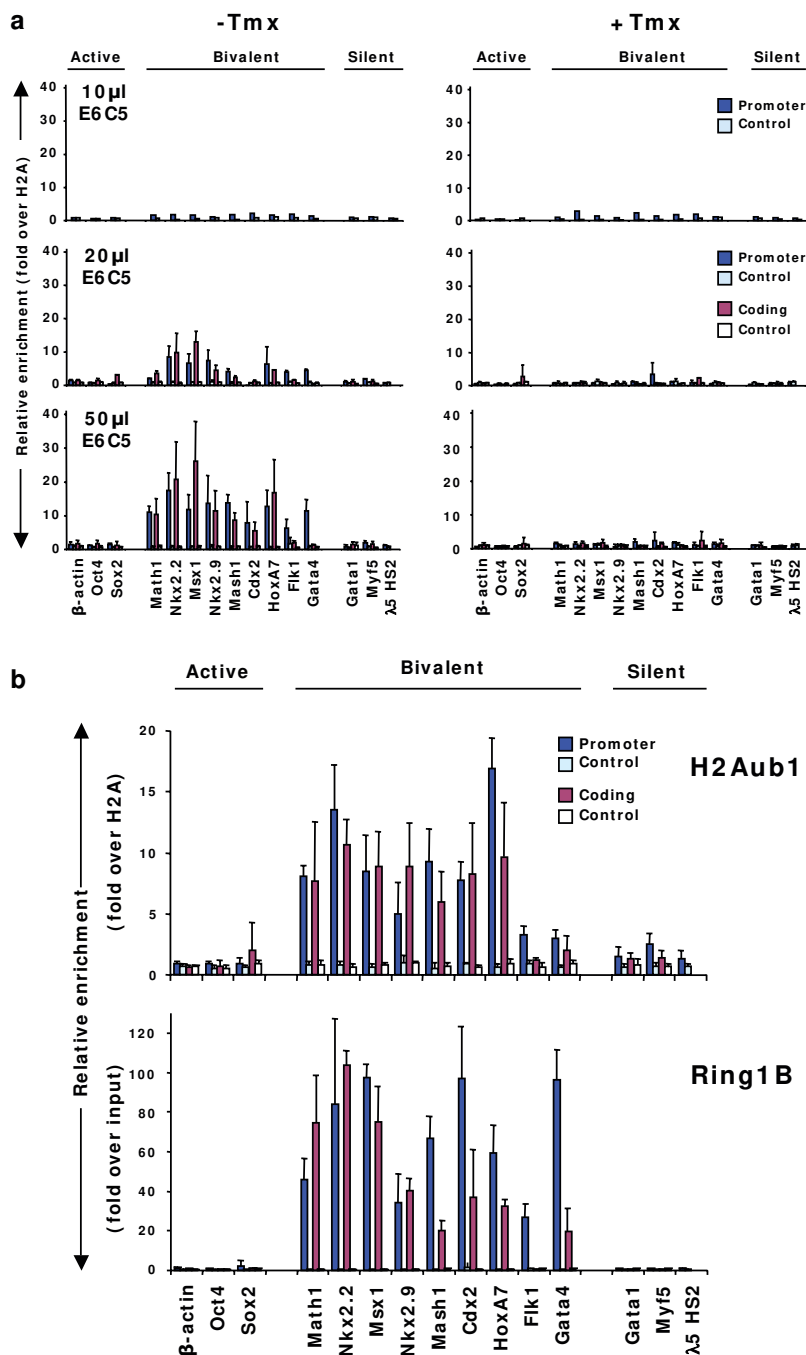


Figure S2 Bivalent genes are marked by Ring1B and H2Aub1. **(a)** Optimising the detection of H2Aub1 using IgM antibody. H2Aub1 ChIP enrichment was optimised by titrating the amount of antibody (E6C5) used with a fixed amount of ES-ERT2 cell chromatin (450 μ g), before and after tamoxifen (Tmx) induction (48h) to excise the *Ring1B* gene. The abundance of H2Aub1 was assessed at the promoter (blue bars) and coding regions (red bars; only for 20 and 50 μ l E6C5) of active, bivalent and silent genes. Increasing the amount of anti-H2Aub1 selectively enhanced the detection of H2Aub1 at bivalent genes (including *HoxA7*, a known PRC1 target), but not at active genes or silent controls. Specificity for H2Aub1 was also confirmed by the consistent loss of binding at bivalent genes in cells lacking Ring1B, with all antibody concentrations. Enrichment is shown relative to input DNA using the same amount of DNA in the PCR and normalised to H2A abundance. Mean and standard deviations are presented from 2 independent experiments for 20 μ l and 4 experiments for 50 μ l; data for 10

μ l originates from a single (paired) experiment. **(b)** The binding of Ring1B and the modification which it catalyses, H2Aub1, were assessed at the promoter (blue bars) and coding regions (red bars) of active, bivalent and silent genes in murine ES-OS25 cells by ChIP and qPCR. In ES-OS25 cells, as in uninduced ES-ERT2 cells, Ring1B and H2Aub1 were found at the promoter and coding regions of bivalent genes, but not at control active or silent genes. H2Aub1 and Ring1B distribution were similar, consistent with the capacity of Ring1 to modify H2A. Enrichment is expressed relative to input DNA using the same amount of DNA in the PCR, and normalized to the levels of histone H2A for H2Aub1. Background levels (mean enrichment from control antibodies and beads alone) at promoter and coding regions are shown as pale blue or white bars, respectively (low level of background not visible for Ring1B). Mean and standard deviations are presented from 3-4 independent experiments.

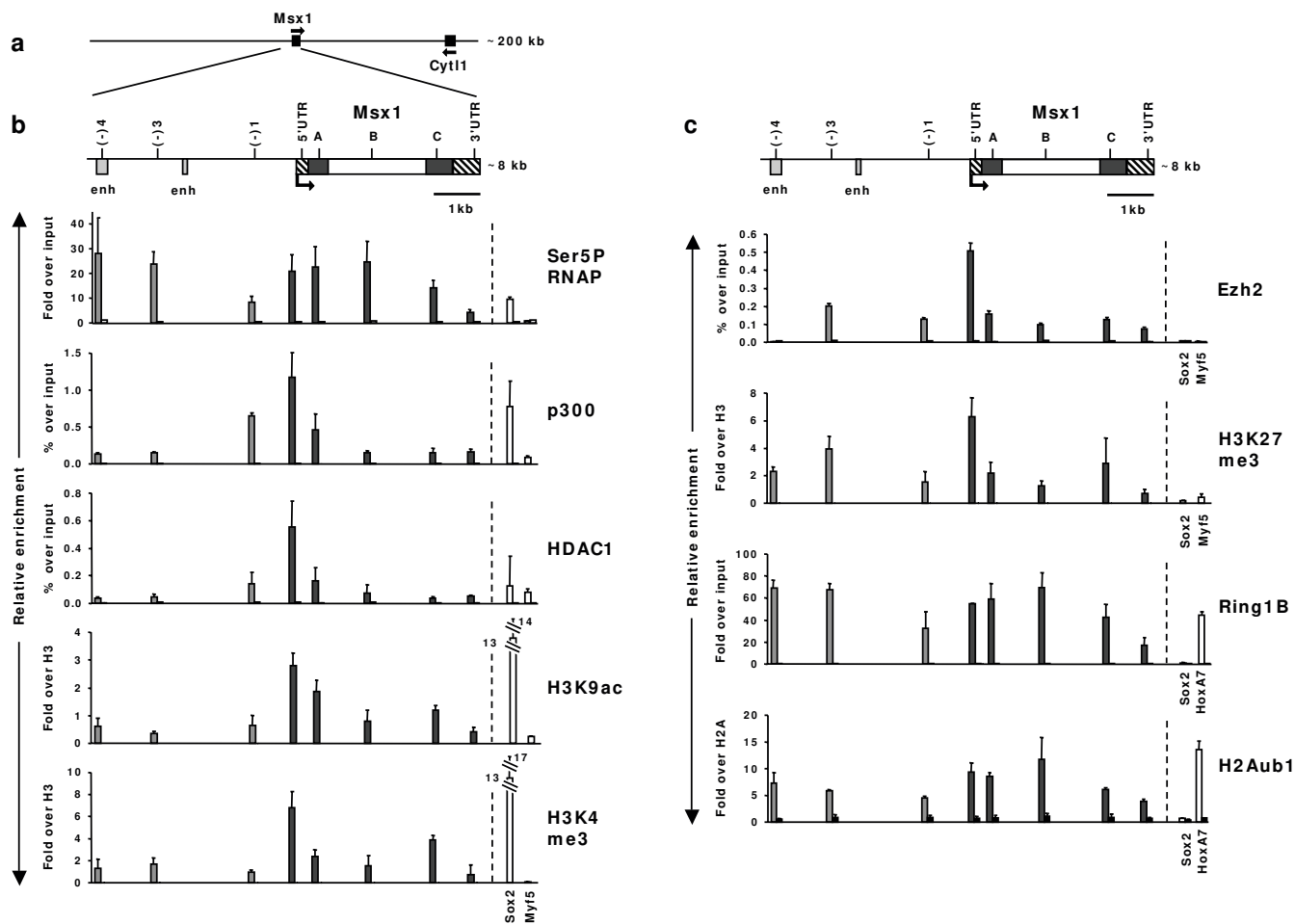


Figure S3 Mapping the binding of transcription machinery and Polycomb repressor components at the *Msx1* locus in ES cells. (a) Diagram illustrating the genomic context of *Msx1* on mouse chromosome 5. *Msx1* is within a gene-poor region (Ensembl v37, Feb 2006); the nearest gene, *Cyt11*, is ~81 kb away. Arrows indicate direction of transcription. (b) ChIP analysis of an 8 kb region of *Msx1* that spans -4.5 kb (upstream of transcription start site; arrow), two enhancer regions at -4.2 kb and -2.4 kb (enh, light grey boxes), and the entire coding region of 3.9 kb containing 2 exons (dark grey boxes). Untranslated regions are depicted by striped boxes. The position of the primers used for ChIP analyses is indicated by name or letter above the line diagram. Ser5P RNAP, p300, HDAC1, H3K9ac and H3K4me3 occupancy across the *Msx1* gene locus was assessed in ES-OS25 cells using ChIP and qPCR. (c) Binding of PRC2 and PRC1 components, Ezh2 and Ring1B, and associated histone modifications, H3K27me3 and H2Aub1, across

the *Msx1* gene locus. Enrichment is shown relative to input DNA using the same amount of DNA in the PCR (for Ser5P, Ring1B, H2Aub1), or relative to total input DNA (for p300, HDAC1, H3K9ac, H3K4me3, H3K27me3, Ezh2), according to the ChIP protocol used to optimise detection. Histone modifications are normalised for unmodified core histones (H3 or H2A). Active (*Sox2*) and silent (*Myf5*) genes were used as controls, except *HoxA7*, a known PRC1 target, which was used as a positive control for Ring1B and H2Aub1. Background levels (mean enrichment from control antibodies and beads alone) for Ser5P, Ring1B, H2Aub1; enrichment from control antibody for p300, HDAC1, H3K9ac, H3K4me3, Ezh2, H3K27me3 are presented (black bars) next to each data point but in most cases are negligible. Mean and standard deviations are presented from 3 independent experiments, except for Ring1B and H2Aub1 which have been performed twice.

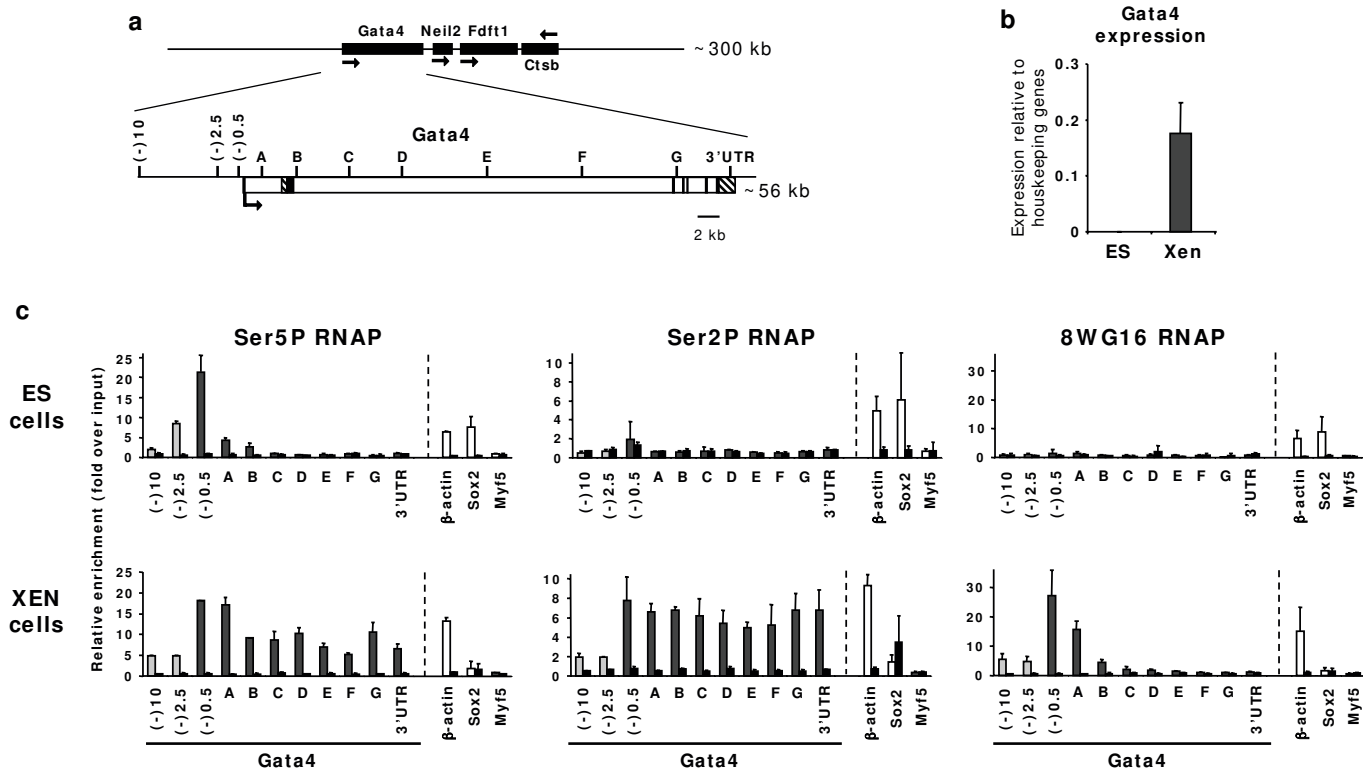


Figure S4 Mapping the binding of different forms of RNAP at the *Gata4* locus in ES and XEN cells. (a) Diagram illustrating the genomic context of *Gata4* on mouse chromosome 14. Arrows indicate direction of transcription. A 56 kb region of *Gata4* that spans -10 kb (upstream of transcription start site; arrow), and the entire coding region of 46.4 kb containing 7 exons (dark grey boxes) was analysed. Untranslated regions are depicted by striped boxes. The position of primer pairs used for ChIP analyses is indicated by name or letter above the line diagram. (b) *Gata4* gene expression was assessed by quantitative RT-PCR in ES and XEN cells. Spliced transcripts were identified using primers located at exon1 and exon2. Mean and standard deviations from 2 independent experiments are represented relative to housekeeping genes. *Gata4* expression in adult heart (not shown, and reference 13) and XEN cells was approximately 1,000 and 600 fold higher, respectively, than in ES cells. (c) Ser5P, Ser2P and 8WG16 RNAP occupancy across the *Gata4* gene locus was assessed in ES-OS25 and

XEN cells, where RNAP is poised and active respectively, using ChIP and qPCR. In ES cells, Ser5P extends into the coding regions of *Gata4* (up to 5 kb), but is not detected at downstream coding regions, while Ser2P and 8WG16-RNAP were not detected. In XEN cells, Ser5P binding peaked at the promoter and extended into the coding regions, while Ser2P was enriched throughout the coding region. 8WG16 binding peaked at the *Gata4* promoter in XEN cells, but was undetected 15 kb downstream of the promoter. Enrichment is shown relative to input DNA using the same amount of DNA in the PCR. Constitutively active, ES cell-specific, and silent genes (β -actin, *Sox2* and *Myf5*, respectively) were used as controls. Coding regions were analysed for Ser2P RNAP, and promoter regions for Ser5P and 8WG16 RNAP. Background levels, mean enrichment from control antibodies and beads alone, are presented (black bars) next to each data point. Values shown are from 2 independent experiments.

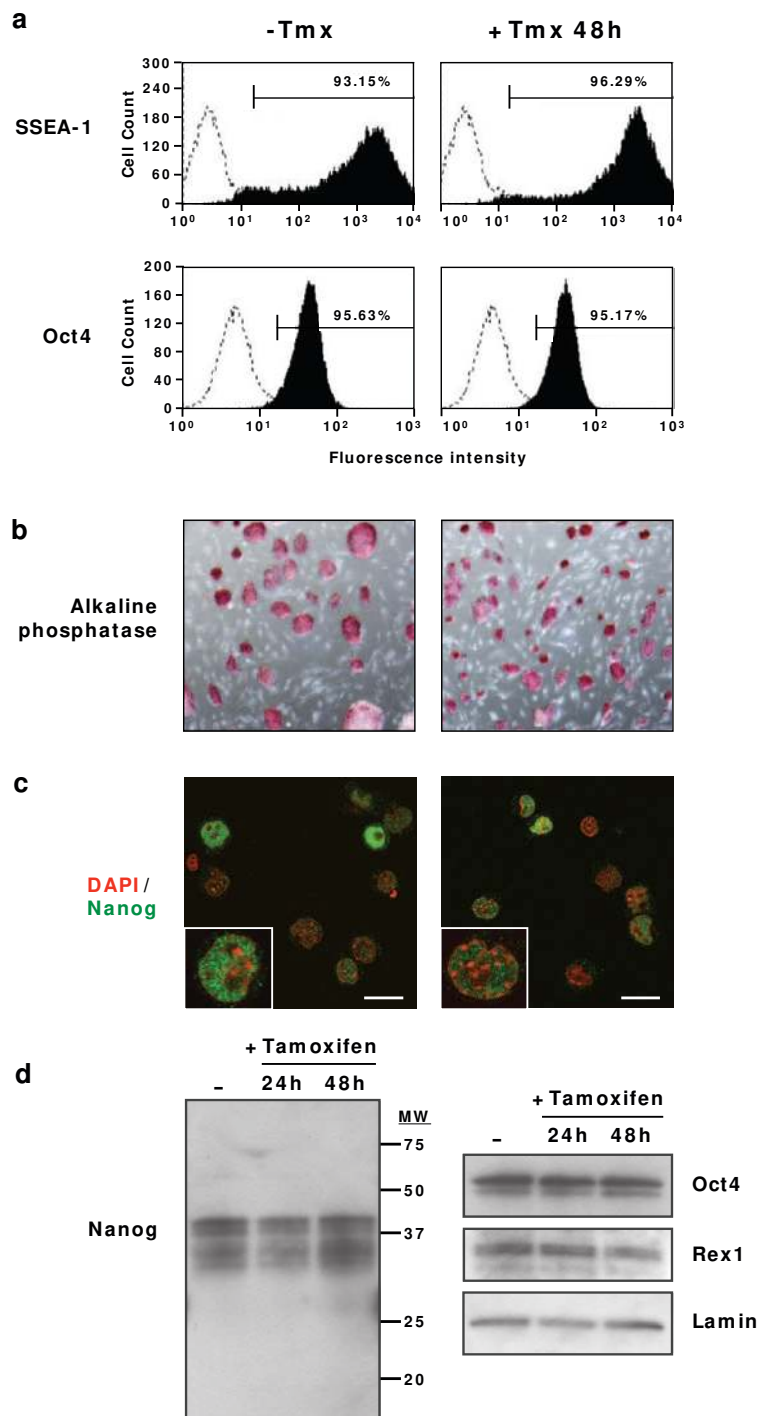


Figure S5 Ring1B conditional knockout ES-Ert2 cells remain undifferentiated 48 hours after tamoxifen induction. **(a)** FACS analyses of SSEA-1 and Oct4 expression in ES-Ert2 cells show that most cells continue to express SSEA-1 and Oct4 proteins at 48 hours of tamoxifen (Tmx) induction. **(b)** Alkaline phosphatase activity is also retained by ES-Ert2 cells 48 hours after Tmx induction. **(c)** Nanog expression is retained by ES-Ert2 cells 48 hours after Tmx treatment. Indirect immunofluorescence analysis of Nanog (green) labeling of nuclei counterstained with DAPI (red) showed Nanog expression in untreated and Tmx-induced cells was similar (approximately 76% versus 64% positive

cells, respectively; $n > 100$, 3 independent experiments). The levels of Nanog protein detected in individual cells were variable, consistent with the reported periodicity of Nanog expression in undifferentiated ES cells¹⁴. Bar, 20 μ m. **(d)** Western blot analysis of nuclear extracts of ES-Ert2 cells confirmed similar levels of Nanog, Oct4 and Rex1 proteins were detected at 0, 24 and 48 hours of Tmx treatment. Western results for lamin levels in the same extracts are shown as a loading control. Full scans of additional western blots that included extracts from primary embryonic fibroblasts (PEF) as a negative control are shown in Supplementary Figure S7. MW, molecular weight markers (kDa).

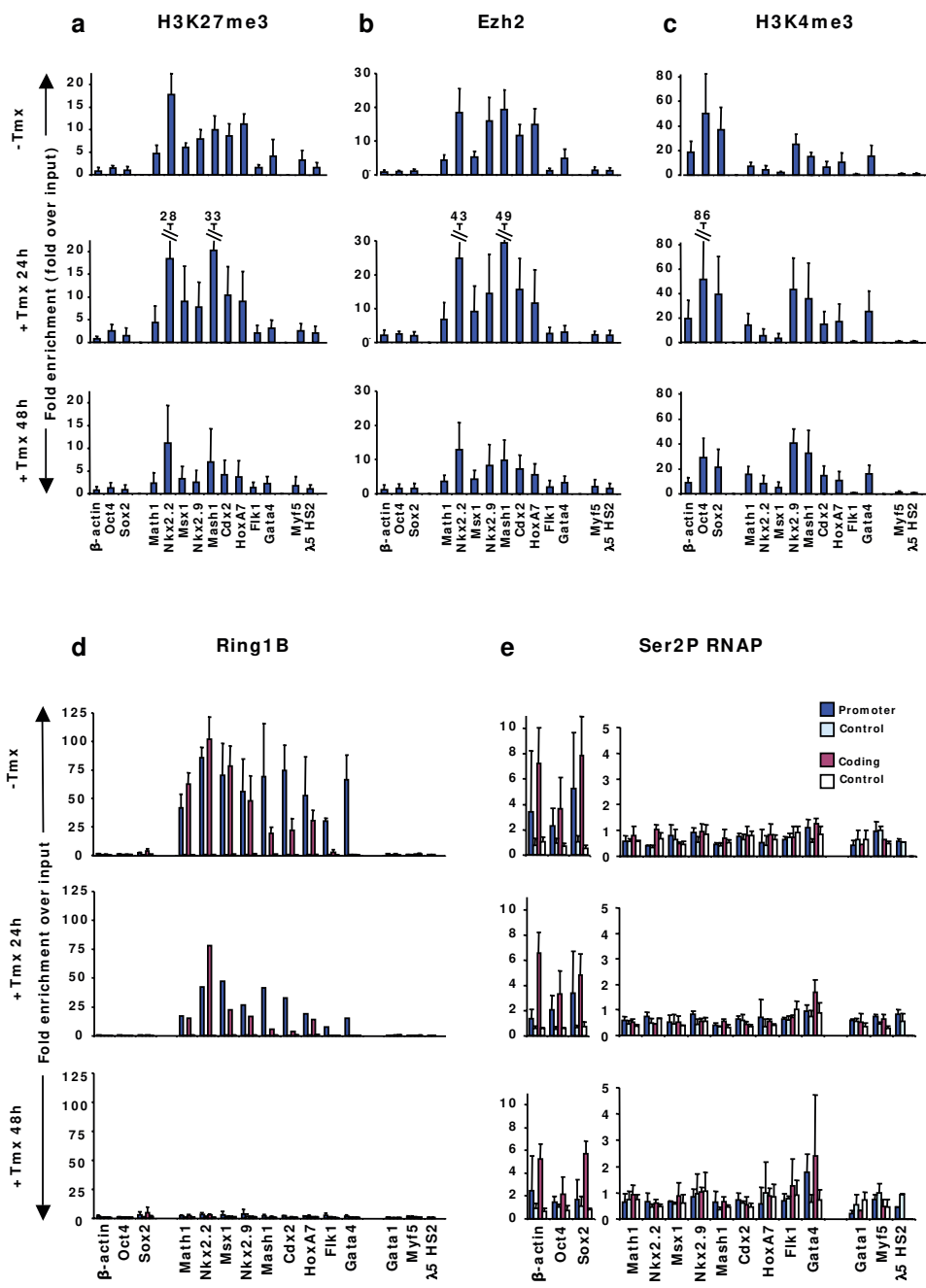


Figure S6. Effect of global Ring1B depletion on histone modifications, recruitment of Ring1B protein and Ser2P RNAP at bivalent genes. The abundance of H3K27me3 (a), Ezh2 (b), H3K4me3 (c), Ring1B (d) and Ser2P RNAP (e) was assessed at the promoter (blue bars) and coding regions (red bars; for Ring1B and Ser2P RNAP) of bivalent genes, after 0, 24 and 48 hours tamoxifen (Tmx) treatment of ES-ERT2 cells to excise the *Ring1B* gene. (a-d) Histone modifications associated with both active and repressive chromatin are simultaneously present at promoters of silent tissue-specific genes in uninduced ES-ERT2 cells, consistent with their bivalent nature in other ES cell lines^{6,15}; low levels of H3K4me3 are observed for *Msx1* and *Flk1*. Ezh2 and Ring1B are found at the promoter (b and d, respectively) and coding regions (not shown and d, respectively) of bivalent genes, but not at active or silent genes. After 48h of Tmx treatment, Ring1B enrichment at bivalent genes is lost; the negative regulators H3K27me3 and Ezh2 show a moderate decrease at bivalent genes, whereas the positive mark H3K4me3 shows a slight increase. (e) In uninduced ES-ERT2 cells, Ser2P RNAP is enriched at active genes but not at bivalent or silent genes, as

seen in ES-OS25 (Fig. 1a) and ES-E14 (not shown), with the exception of *Gata4* which shows a low level of Ser2P in the coding region. Upon *Ring1B* excision, Ser2P is unchanged at all genes except *Gata4*, where slight increases are seen in both the promoter and coding regions. Enrichment is represented either relative to input DNA using the same amount of DNA in the PCR (Ring1B, Ser2P), or relative to total input DNA (H3K27me3, Ezh2, H3K4me3), depending on the optimal ChIP protocol for each protein or modification. Mean and standard deviations are presented from 4 independent ChIP experiments, except Ring1B values which are from 3 (-Tmx and +Tmx 48h) or one (+Tmx 24h; paired) independent experiments. Background levels (d,e; mean enrichment from control antibodies and beads alone) at promoter and coding regions are shown as pale blue or white bars, respectively (low level of background not visible for Ring1B). Differences in abundance of H3K27me3, Ezh2 and Ring1B at bivalent genes over time were statistically significant ($p < 0.0001$, $p = 0.01$ and $p < 0.0001$, respectively; ANOVA), whilst variation in H3K4me3 and Ser2P RNAP levels were not ($p = 0.91$ and $p = 0.14$, respectively; ANOVA).

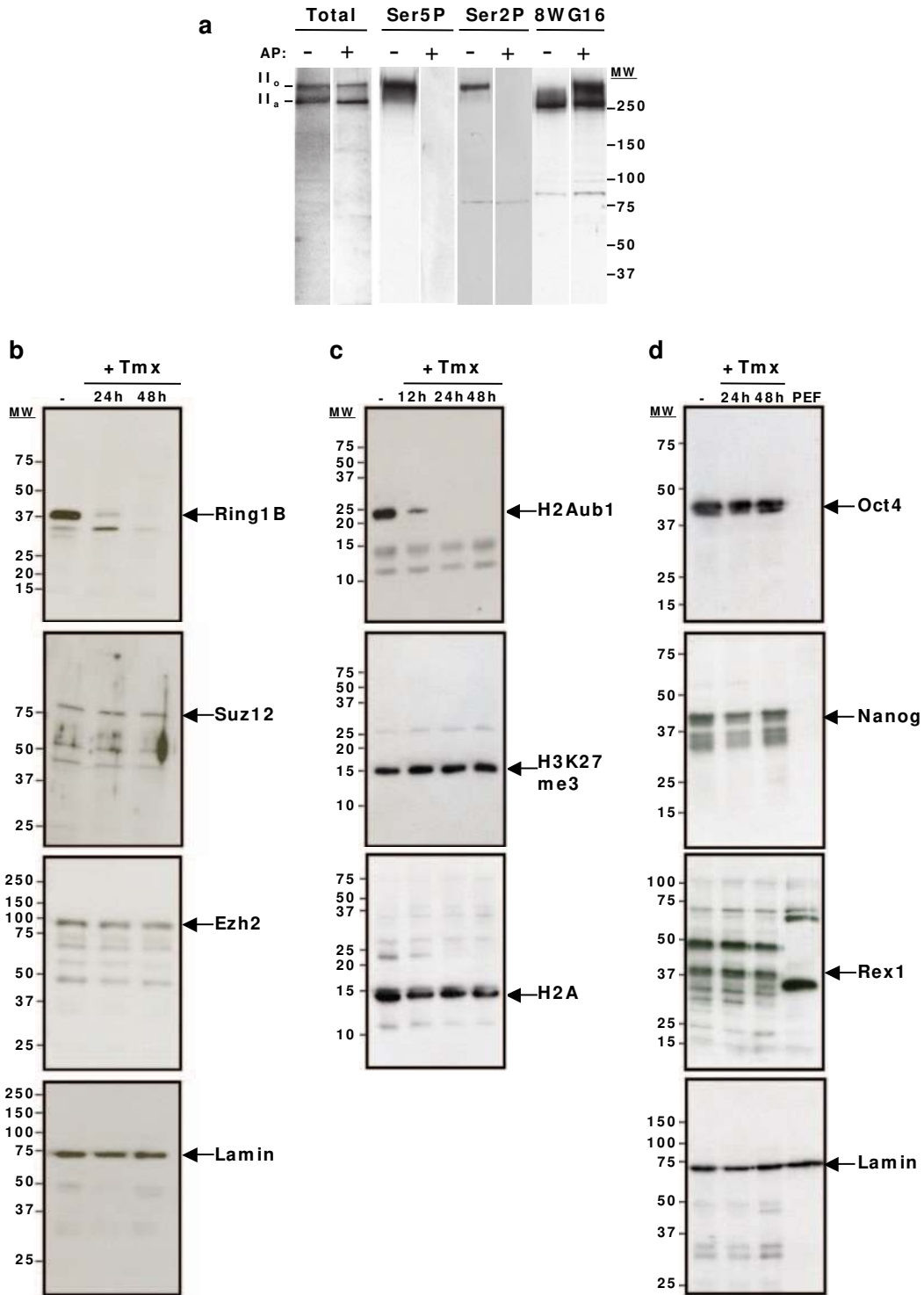


Figure S7 Full-length blot scans for western blots. **(a)** Reactivity of different RNAP antibodies against hyper- (II_o) and hypo-phosphorylated (II_a) forms of the largest subunit of RNAP, RPB1, assessed by western blotting. Whole cell extracts were prepared from ES-OS25 cells. Treatment of membranes with alkaline phosphatase (AP) prior to western blotting reveals sensitivity of antibodies to phosphorylated epitopes. Full-length blot scans of results presented in Figure 1b. **(b)** Western blot analyses of nuclear extracts of ES-Ert2 cells cultured with 800 nM tamoxifen (Tmx) for 0-48 hours, using anti-Ring1B, anti-Suz12, anti-Ezh2, and anti-Lamin (loading control) antibodies. Full-length blot scans of results presented in Figure 4c.

(c) Western blot of acid-extracted histones from ES-Ert2 cells cultured with 800 nM Tmx for 0-48 hours, using anti-H2Aub1, anti-H3K27me3 and anti-H2A (loading control) antibodies. Full-length blot scans of results presented Figure 4d. **(d)** Western blot analysis of nuclear extracts of ES-Ert2 cells confirmed similar levels of Nanog, Oct4, Rex1 and Lamin (loading control) proteins were detected at 0, 24 and 48 hours of Tmx treatment. Repeat experiments showing full-length blot scans of western blot analyses presented in Supplementary Figure S5, including extracts from primary embryonic fibroblasts (PEFs). MW, molecular weight markers (kDa).

Table S1 Antibodies used for ChIP and western blot analyses.

Antibody against	Clone	Raised in (isotype)	Volume used in ChIP (per IP)	Working dilution for Westerns	Origin
RNAP					
N-terminus (amino acids 1-224) of RPB1	H224 (sc-9001x)	Rabbit (IgG)	25 µl (50 µg)	1:200	Santa Cruz Biotechnology
RPB1 CTD phosphorylated on Ser2	H5 (MMS-129R)	Mouse (IgM)	50 µl (50 µg)	1:500	Covance, Princeton, NJ
RPB1 CTD phosphorylated on Ser5	CTD4H8 (05-623)	Mouse (IgG)	10 µl (25 µg)	1:200,000	Upstate/Millipore
Non-phosphorylated RPB1 CTD	8WG16* (MMS-126R)	Mouse (IgG)	10 µl (25 µg)	1:200	Covance
Histones and modifications					
Ubiquityl-Histone H2A	E6C5 (05-678)	Mouse (IgM)	50 µl	1:400	Upstate/Millipore
Acetyl-Histone H3 (Lys9)	07-352	Rabbit (IgG)	0.5 µg	-	Upstate/Millipore
Acetyl-Histone H4	06-866	Rabbit (IgG)	0.5 µg	-	Upstate/Millipore
Dimethyl-Histone H3 (Lys4)	07-030	Rabbit (IgG)	0.5 µg	-	Upstate/Millipore
Trimethyl-Histone H3 (Lys4)	ab8580	Rabbit (IgG)	0.5 µg	-	Abcam Ltd, Cambridge, UK
Trimethyl-Histone H3 (Lys 4)	07-473	Rabbit (IgG)	5 µl	-	Upstate/Millipore
Trimethyl-Histone H3 (Lys27)	07-449	Rabbit (IgG)	0.5 µg	1:500	Upstate/Millipore
Histone H2A	07-146 (acidic patch)	Rabbit (IgG)	10 µl	1:500	Upstate/Millipore
Histone H3-carboxyterminal	ab1791	Rabbit (IgG)	0.5 µg	-	Abcam Ltd
Polycomb components					
Ezh2	07-689	Rabbit (IgG)	5 µl	1:1000	Upstate/Millipore
Ring1B	-	Mouse (IgG, hybridoma)	30 µl	1:500	Ref. ¹⁰
Suz12	ab12073	Rabbit (IgG)	-	1:1000	Abcam Ltd
Transcription machinery components					
Histone deacetylase (HDAC) 1	06-720	Rabbit (IgG)	2 µg	-	Upstate/Millipore
p300/CBP	C-20 (sc-585)	Rabbit (IgG)	2 µg	-	Santa Cruz Biotechnology
Other					
Nanog	REC-RCAB 0002PF	Rabbit (IgG)	-	1:50	Cosmo Bio Co. Ltd, Tokyo, Japan
Oct-3/4	N-19 (sc-8628)	Goat (IgG)	-	1:1000	Santa Cruz Biotechnology
Rex1	ab28141	Rabbit (IgG)	-	1:100	Abcam Ltd
Controls					
Digoxigenin	200-002-156	Mouse (IgG)	10 µl (13 µg)	-	Jackson ImmunoResearch Technologies, West Grove, PA
Glutathione-S-Transferase	59258	Rabbit (IgG)	30 µl	-	MP Biochemicals, Irvine, CA
5T _γ -3H12 membrane protein	-	Mouse (IgM)	30 µl	-	IGBMC, Strasbourg, France
Hemagglutinin (HA)	Y-11 (sc-805)	Rabbit (IgG)	2.5 µl	-	Santa Cruz Biotechnology
Lamin B	C-20 or M-20 (sc-6216/7)	Goat (IgG)	-	1:1500	Santa Cruz Biotechnology

Supplementary Information

Table S2 List of primers used in ChIP and RT-PCR analyses in 5' to 3' orientation. (*) Indicates primers with two designations for their use in promoter and coding region analyses (e.g. Figure 1a) and in the detailed mapping of single genes (e.g. Figure 3).

ChIP primers	
β-actin promoter F	GCAGGCCTAGTAACCGAGACA
β-actin promoter R	AGTTTTGGCGATGGGTGCT
β-actin coding F	TCCTGGCCTCACTGTCCAC
β-actin coding R	GTCCGCCTAGAAGCACTTGC
Oct4 promoter F	GGCTCTCCAGAGGATGGCTGAG
Oct4 promoter R	TCGGATGCCCCATCGCA
Oct4 coding F	CCTGCAGAAGGAGCTAGAACA
Oct4 coding R	TGTGGAGAAGCAGCTCCTAAG
Sox2 promoter F	CCATCCACCCTTATGTATCCAAG
Sox2 promoter R	CGAAGGAAGTGGGTAAACAGCAC
Sox2 coding F	GGAGCAACGGCAGCTA
Sox2 coding R	GTAGCGGTGCATCGGT
Math1 promoter F	CCTTCTTTGACTGGGCAGAC
Math1 promoter R	ACTCGGAGATCGCACACC
Math1 coding F	CCAGTTGCCATTGCTTTAT
Math1 coding R	AGGATACTAGATTTGCAACATTCTT
Nkx2.2 (-3.5 kb) F	TAACGCTTTGGAAGCAGACGTG
Nkx2.2 (-3.5 kb) R	GCACTGGGCAGCTAGACTAGGA
Nkx2.2 (-2.5 kb) F	CAGAGAGCCCCAGCCTGAAA
Nkx2.2 (-2.5 kb) R	TCCCTTTCCCTTGCAAGA
Nkx2.2 (-1 kb) F	CGAACCCCTGCCACTGCTAGA
Nkx2.2 (-1 kb) R	AGAGGAATAGGCTTGGACATG
Nkx2.2 promoter (5'UTR) * F	CAGGTTCTGTGAGTGGAGCCC
Nkx2.2 promoter (5'UTR) * R	GCGCGGCCTCAGTTTGTAAC
Nkx2.2 (A) F	GTCGCTGACCAACACAAAGACG
Nkx2.2 (A) R	TGTCGTAGAAAGGGCTCTTAAGGG
Nkx2.2 (B) F	ACTATGTGGTGCCTGACGCG
Nkx2.2 (B) R	AAACAGTTTCCTCTTTGGAGAGACGT
Nkx2.2 (C) F	CGCTGCGCAGACTCTCCTCT
Nkx2.2 (C) R	GAAGAGAAGCGCATCAGGCG
Nkx2.2 coding (D) * F	AGAGCCCTCGGCTGACGAGT
Nkx2.2 coding (D) * R	CGTGAGACGGATGAGGCTGG
Nkx2.2 (E) F	ACCTTCCAGGCAGGCATCCC
Nkx2.2 (E) R	CGGCGCTACCAAGTCCACT
Nkx2.2 (F) F	TGCGTACCAAGTTGAGGCCTAGT
Nkx2.2 (F) R	AAGAGGAATGACCAGTTTGGAGGA
Nkx2.2 (G) F	AAAGTATGCCAACTCGGTGCCA
Nkx2.2 (G) R	GGAAGATAATCTTCTGGGCTCCCA
Nkx2.2 (3'UTR) F	GGATGGATGCCAGGATCGAA
Nkx2.2 (3'UTR) R	GCATTGTGGTCCTACTGTAAATGGAC
Msx1 promoter F	ACAGAAAGAAATAGCACAGACCATAAGA
Msx1 promoter R	TTCTACCAAGTTCCAGAGGGACTTT
Msx1 coding F	AGATGGCCGCGAAAC

Msx1 coding R	CCAGAGGCACTGTAGAGTGA
Msx1 (-4 kb) F	ATTTCGTAGGCAGCAAAGTGGT
Msx1 (-4 kb) R	GGACTTGAGGGCGCACTT
Msx1 (-3 kb) F	CCGTGAGATAACAGGCCCAGC
Msx1 (-3 kb) R	GCCATGTGGCTCATTCCCGA
Msx1 (-1 kb) F	CGGTCTTCACCCAAGGCATCCAG
Msx1 (-1 kb) R	GGTCCTGTTGGTTCTGTGGGTACGG
Msx1 (5'UTR) F	CGCTGCCACGCTGGCCTTGCCCTTAT
Msx1 (5'UTR) R	TCTGCGAGCTCCTGGGTTCCCTGGCC
Msx1 (A) F	CTTCAGCGTGGAGGCCCTCA
Msx1 (A) R	CTGAGAAATGGCCGAGAGGC
Msx1 (B) F	TGGCGTGATGCTGAGGAACG
Msx1 (B) R	CCAGGCCGCCCTAAAGAAGG
Msx1 (C) F	GCTGGCTCTGGAGCGCAAGT
Msx1 (C) R	AGCTCCGCCTCCTGCAGTCT
Msx1 (3'UTR) F	ATTGCTCTGAGGGGGCAGGGCGCAT
Msx1 (3'UTR) R	GGGATGCTTGAGAGCCACGA
Nkx2.9 promoter F	TGGCACCTTCCGGACTTG
Nkx2.9 promoter R	AAGTGCGAGGCGCTCG
Nkx2.9 coding F	AGCTCTGGTCTCCTGGAAC
Nkx2.9 coding R	GTGTGTGTTTGCCGGTTAG
Mash1 promoter F	CCAGGCTGGAGCAAGGGA
Mash1 promoter R	CGGTTGGCTTCGGGAGC
Mash1 coding F	CCAGAATGACTTCAGCACCA
Mash1 coding R	AGGCAACCTATGGGAACCAA
Cdx2 promoter F	GGACTCCGCGAGCCAA
Cdx2 promoter R	CTCAGCCCACGGTGCTC
Cdx2 coding F	CCAATGACTGATGGATTGTAGTT
Cdx2 coding R	GCTCACTTTTCTCCTGATG
HoxA7 promoter F	GAGAGGTGGGCAAAGAGTGG
HoxA7 promoter R	CCGACAACCTCATACCTATTCTG
HoxA7 coding F	CTGGACCTTGATGCTTCTAACT
HoxA7 coding R	AGCCAGAGAAAGAGGGATTCTA
Flk1 promoter F	CCACCCCTCCCGGTAA
Flk1 promoter R	GGTCCGCGCGATCTAA
Flk1 coding F	TTCATGGACCCAAAGACTAC
Flk1 coding R	GTTCTCGGTGATGTACACG
Gata4 (-10 kb) F	TTGGTGTGCCAGAAGCATT
Gata4 (-10 kb) R	TTCCCCCTTGAAATTGAGTCT
Gata4 (-2.5 kb) F	TCGCCTAGTTCTGGTTCCA
Gata4 (-2.5 kb) R	GTCAAACCAGACGCGTTTT
Gata4 promoter (-0.5 kb) * F	AAGAGCGCTTGCGTCTCTA
Gata4 promoter (-0.5 kb) * R	TTGCTAGCCTCAGATCTACGG
Gata4 coding (A) * F	TTGCACATTAACACCACACGTATA
Gata4 coding (A) * R	CCACCATTCAATTTTTAAGTCAAGTA
Gata4 (B) F	TATCTGGGATTGAGCCCTTACTTC
Gata4 (B) R	ACCCTGGGGGATCCTCTAAC
Gata4 (C) F	TGAGCCACTTGAAATACTATGTT
Gata4 (C) R	TTTACCTAGGGCCCAATGAA
Gata4 (D) F	TTCATGGGCCTGGTATCC
Gata4 (D) R	GTGTAAGTGGCTCAAAGTCACC

Gata4 (E) F	GGGGTGAATCTTGGGATGTT
Gata4 (E) R	GCCTCTTATCCCAAGTTGGATTAT
Gata4 (F) F	GAAAACACGATGCAATGGTAGATA
Gata4 (F) R	AGCGAACCAGTTCCTGAAAG
Gata4 (G) F	ACTTGCACTCGCTCCAAAGAT
Gata4 (G) R	GGTTACGTTGGCTTTCGAGAC
Gata4 (3'UTR) F	CAAAGTGCTGGGTTCAATGC
Gata4 (3'UTR) R	CAGGCTGCGATTGATGAA
Gata1 promoter F	AGAGGAGGGAGAAGGTGAGTG
Gata1 promoter R	AGCCACCTTAGTGGTATGACG
Gata1 coding F	TGGATTTTCCTGGTCTAGGG
Gata1 coding R	GTAGGCCTCAGCTTCTCTGTAGTA
Myf5 promoter F	GGAGATCCGTGCGTTAAGAATCC
Myf5 promoter R	CGGTAGCAAGACATTAAGTTCCGTA
Myf5 coding F	GATTGCTTGTCCAGCATTGT
Myf5 coding R	AGTGATCATCGGGAGAGAGTT
λ5 promoter	AGGCCCTAACAGCTTCACTACTC
λ5 promoter	GCATCTGGGCCTCGGTTTA
λ5 HS2	ACCCAGTAAGCAAGTTTCA
λ5 HS2	ATAAGCTCTCCTCCCTCAAG
Expression primers (spliced transcripts)	
β-actin F	TCTTTGCAGCTCCTTCGTTG
β-actin R	ACGATGGAGGGGAATACAGC
Oct4 F	ACCTCAGGTTGGACTGGGCCTA
Oct4 R	GCCTCGAAGCGACAGATGGT
Math1 F	GGAGAAGCTTCGTTGCACGC
Math1 R	GGGACATCGCACTGCAATGG
Nkx2.2 F	TGTGCAGAGCCTGCCCTTAA
Nkx2.2 R	GCCCTGGGTCTCCTTGTCAT
Msx1 F	GCCTCTCGGCCATTTCTCAG
Msx1 R	CGGTTGGTCTTGTGCTTGCG
Nkx2.9 F	GGCCACCTCTGGACGCCTCG
Nkx2.9 R	GCCAGCTGCGACGAGTCTGC
Mash1 F	TGGAGACGCTGCGCTCGGC
Mash1 R	CGTTGCTTCAATGGAGGCAAATG
Cdx2 F	CAGCCGCCGCCACAACCTTCCC
Cdx2 R	TGGCTCAGCCTGGGATTGCT
HoxA7 F	AAGCCAGTTTCCGCATCTACC
HoxA7 R	GTAGCGGTTGAAATGGAATTCC
Fli1 F	AGGGGAACTGAAGACAGGCTA
Fli1 R	GATGCTCCAAGGTCAGGAAGT
Gata4 F	GAGGCTCAGCCGAGTTGCAG
Gata4 R	CGGCTAAAGAAGCCTAGTCCTTGCTT
Gata1 F	GTCCTCACCATCAGATTCCACAG
Gata1 R	AGTGGATACACCTGAAAGACTGGG
Myf5 F	GGAGATCCTCAGGAATGCCATCCGC
Myf5 R	GACGTGATCCGATCCACAATGCTGG
Expression primers (5' transcripts)	
β-actin F	CCACCCGCGAGCACA
β-actin R	CCGGCGTCCCTGCTTAC
Oct4 F	TGAGCCGTCTTTCCACCA
Oct4 R	TGAGCCTGGTCCGATTCC

Math1 F	TGTGCGATCTCCGAGTGA
Math1 R	CTCGGAGGTGCCGTGTTA
Nkx2.2 F	CGCTGCGCAGACTCTCCTCT
Nkx2.2 R	GAAGAGAAGCGCATCAGGCG
Msx1 F	CGCTCGAGTTGGCCTTCT
Msx1 R	CGGAGTCCTCCACTTTGACAC
Nkx2.9 F	GTGCGCAGCCTCCTGAAT
Nkx2.9 R	GGTCCCTCCTCCGCACTC
Cdx2 F	ATCCCCGCCTCTACAGTTACT
Cdx2 R	CGCAGGGGGCTAGAGATAAA
Gata4 F	GGACTCACGGAGATCGCG
Gata4 R	GGACTCGGGGAACCCTACC
Myf5 F	GGAATATATAAAGAGCCCCAACC
Myf5 R	TTTGGGACTGTCTCTCTGTAATTAAC

Supplementary Methods

Cell culture

ES-OS25 and ES-ZHBTc4 (kindly donated by A. Smith) cells were grown on 0.1% gelatin-coated surfaces in supplemented GMEM-BHK21 as described previously^{1,2}. E14 cells were cultured in DMEM supplemented with 10% distilled water, 15% FCS, 2 mM L-glutamine, 1% MEM non-essential amino acids, 50 μ M 2-mercaptoethanol (all from Gibco, Invitrogen, Paisley UK), and 2,400 U/ml of leukemia inhibitory factor (LIF, Chemicon, Millipore, Chandler's Ford, UK) in 0.1% gelatin-coated flasks. ES-ERT2 *Ring1A*^{-/-} cells were maintained in an undifferentiated state by co-culture on mitomycin-inactivated mouse embryonic fibroblasts on 0.1% gelatin-coated flasks in DMEM supplemented with non-essential amino acids, 50 μ g/ml penicillin and streptomycin, 2 mM L-glutamine, 0.1 mM 2-mercaptoethanol (all from Gibco), 20% FCS (Autogen Bioclear, Calne, UK) and LIF conditioned medium (1,000 U/ml). TS-B1 cells were grown as described previously³. XEN-IM8A1⁴ cells (kindly donated by J. Rossant) were cultured in RPMI 1640 supplemented with 2 mM L-glutamine, 50 μ g/ml penicillin and streptomycin, 1 mM sodium pyrovate, 0.1 mM 2-mercaptoethanol (all from Gibco), and 20% FCS (Globepharm, Guildford, UK), on 0.1% gelatin-coated flasks.

For the *Ring1B* conditional deletion, ES-ERT2 cells were plated feeder-free on gelatin-coated plates 12h before supplementing the medium with 800 nM 4-hydroxytamoxifen (H7904, Sigma, Poole, UK).

For the inhibition of CDK9 and RNAP Ser2 phosphorylation, ES-OS25 cells were treated (1h) with 0.1-100 μ M flavopiridol (from 50 mM stock in DMSO; a kind gift from Sanofi-Aventis, provided by Drug Synthesis and Chemistry Branch, Developmental Therapeutics Program, Division of Cancer Treatment and Diagnosis, National Cancer Institute, Bethesda, MD).

To inhibit RNAP transcription, ES-OS25 cells were treated (7h) with 75 μ g/ml α -amanitin (Sigma). This concentration and incubation time was previously determined by immunofluorescence using H5 antibody (Ser2P RNAP) to monitor the disappearance of productive transcription, and quantitative RT-PCR using primers that amplify *β -actin* primary transcripts (not shown).

Antibodies

Antibodies used for chromatin immunoprecipitation and western blotting, including control antibodies, are presented in Supplementary Information, Table S1.

Chromatin immunoprecipitation for RNAP, H2Aub1 and Ring1B

Chromatin immunoprecipitation (ChIP) was performed for RNAP, Ring1B and H2Aub1 (anti-ubiquityl-H2A, clone E6C5; Upstate, Watford, UK) as described previously⁵, with some modifications.

Details of antibodies are shown in Supplementary Information, Table S1. Control antibodies were mouse IgG anti-digoxigenin, rabbit anti-glutathione-S-transferase, and mouse IgM 5T γ -3H12. H2Aub1 ChIP was optimized by titrating the amount of antibody for a fixed amount of chromatin (450 μ g chromatin; see Supplementary Information, Fig. S2a). Fifty microlitre of antibody were used in Figs. 2c, 5, and Supplementary Information, Fig. S2b, S3c.

Cells were treated with 1% formaldehyde (37°C, 10 min) and the reaction stopped with addition of glycine to a final concentration of 0.125 M. Cells were washed in ice-cold PBS, before “swelling” buffer (25 mM HEPES pH 7.9, 1.5 mM MgCl₂, 10 mM KCl and 0.1% NP-40) was added to lyse the cells (10 min, 4°C). Cells were scraped from flasks, and nuclei isolated by Dounce homogenization (50 strokes, “Tight” pestle) and centrifugation. After resuspension in “sonication” buffer (50 mM HEPES pH 7.9, 140 mM NaCl, 1 mM EDTA, 1% Triton X-100, 0.1% Na-deoxycholate and 0.1% SDS), nuclei were sonicated to produce DNA fragments with a length of <1.6 kb (see Supplementary Information, Fig. S1c) using a Diagenode Bioruptor (Liege, Belgium; full power; 1h: 30s ‘on’, 30s ‘off’; 4°C). The resulting material was centrifuged twice (4°C, 15 min) at 14,000 rpm. Swelling and sonication buffers were supplemented with 5 mM NaF, 2 mM Na₃VO₄, 1 mM PMSF, and protease inhibitor cocktail (Roche, Burgess Hill, UK).

Protein-A-agarose (Sigma) and protein-G-sepharose beads (Amersham Biosciences, Chalfont St.Giles, UK) were blocked (4°C, >1h) with 1 mg/ml sonicated salmon sperm DNA and 1 mg/ml BSA and washed twice in

sonication buffer prior to use. Goat anti-mouse IgM-agarose beads were not blocked prior to use (Sigma; kind advice from Stephen Buratowski; personal communication).

For ChIP with mouse or rabbit IgG antibodies, chromatin was pre-cleared (4°C, 2h) with appropriate beads in the presence of 0.05 mg/ml BSA, 5 mM NaF, 2 mM Na₃VO₄, 1 mM PMSF, and protease inhibitor cocktail. Approximate chromatin concentrations were obtained by measuring absorbance (280 nm) of alkaline-lysed, crosslinked chromatin, and converted into arbitrary chromatin mass units using the conversion 50 mg/ml for 1 absorbance unit. Pre-cleared chromatin (500-800 µg) was immunoprecipitated (overnight, 4°C) with 10-50 µg of antibody on a rotating wheel. Blocked beads were incubated (4°C, 3h) with antibody-chromatin complexes, washed (1x) with sonication buffer, (1x) sonication buffer containing 500 mM NaCl, (1x) 20 mM Tris pH 8.0, 1 mM EDTA, 250 mM LiCl, 0.5% NP-40 and 0.5% Na-deoxycholate, and (2x) TE buffer (1 mM EDTA, 10 mM Tris HCl pH 8.0).

For ChIP using mouse IgM antibodies H5 and H2Aub1, 450-800 µg of chromatin were combined directly with the antibody and anti-mouse IgM agarose beads, and incubated overnight at 4°C. The beads were then washed twice in sonication buffer; once in 2 mM Tris pH 8.0, 0.02 mM EDTA, 50 mM LiCl, 0.1% NP-40 and 0.1% Na-deoxycholate; and once in TE buffer.

Immune complexes were eluted (5 min, 65°C; and 15 min, room temperature) with 50 mM Tris pH 8.0, 1 mM EDTA and 1% SDS. The elution was repeated and eluates pooled. Reverse cross-linking was carried out (16h, 65°C) with the addition of NaCl and RNase A to final concentrations 160 mM and 20 µg/ml, respectively. EDTA was increased to a final concentration of 5 mM and samples incubated (2h, 45°C) with 200 µg/ml proteinase K. DNA was recovered by phenol-chloroform extraction and ethanol precipitation. The final DNA concentration was determined by PicoGreen fluorimetry (Molecular Probes, Invitrogen) and 0.5 ng of immunoprecipitated and input DNA were analyzed by quantitative real-time PCR (qPCR). Amplifications (40 cycles) were performed using SensiMix NoRef (Quantace, London, UK) with DNA Engine Opticon 1/2 RT-PCR system (BioRad, Hemel Hempstead, Hertfordshire, UK).

RNAP, Ring1B and H2Aub1 ChIP were quantified as described previously⁵. IP or control “cycle over threshold” (Ct) values from the quantitative PCR (IP or control Ct) were subtracted from the input Ct values (Input Ct). This figure was converted into the fold enrichment by $2^{(\text{input Ct} - \text{IP or control Ct})}$. Primer sequences are available upon request.

ChIP for H3 histone modifications, transcription factors and Ezh2

ChIP for H3 histone modifications, transcription factors and Ezh2 was performed as previously described⁶, with minor modifications.

Chromatin fragmented to an average size of 250-500 bp was incubated (1-2h, 4°C) with 30 μ l of blocked protein-A-agarose beads (Upstate) or protein-A/G-PLUS-agarose beads (Santa Cruz Biotechnology, Santa Cruz, CA), on a rotating wheel. Pre-cleared chromatin (150 μ g) was immunoprecipitated (overnight, 4°C) using the antibodies described in Supplementary Information, Table S1. Control antibodies were rabbit anti-mouse IgG or anti-hemagglutinin. Immunocomplexes were eluted and the precipitated DNA was resuspended in 100 μ l TE buffer.

For p300 and HDAC1 ChIP, fixed cell suspension was washed (10 min, 4°C) with 10 mM Tris-HCl, 10 mM EDTA, 0.5 mM EGTA, 0.25% Triton X-100 (pH 8.0), centrifuged and then washed again (10 min, 4°C) with 10 mM Tris-HCl, 200 mM NaCl, 1 mM EDTA, 0.5 mM EGTA, 0.01% Triton X-100 (pH 8.0). Nuclei were resuspended in TEE (10 mM Tris-HCl, 1 mM EDTA, 0.5 mM EGTA pH 8.0), and sonicated and processed as described before.

Quantification of the precipitated DNA was performed using qPCR amplification. The amount of DNA precipitated by each antibody was normalized against 1/10 of the starting input material.

Statistical analysis

Statistical analyses were performed using factorial analysis of variance (ANOVA) in SAS software (v9.2). To preserve the assumption of constant variance and normality of residuals, response variables were transformed into logarithms. Factors were ‘replicate’, ‘gene type’ (active, bivalent, silent), ‘gene region’ (promoter, coding) and ‘time in tamoxifen’ (0, 24, 48h).

Western blot analysis

Whole cell extracts for RNAP westerns were prepared by lysing cells in ice-cold “lysis” buffer⁷, scraping, and shearing the DNA by passage through a 25G needle. Cell lysate (0.5 µg total protein for 4H8 antibody and 5 µg for all other RNAP antibodies) were resolved on 7.5% SDS-PAGE gels. To dephosphorylate RPB1 after electrophoresis and transfer, membranes were incubated (1h, 37°C) in 0.1 U/µl alkaline phosphatase in NEB buffer 3 (New England Biolabs, Hitchin, UK) prior to blocking. Nuclear and histone extracts were prepared as described previously^{8,9}. Nuclear extracts (20 µg) or histone extracts (5 µg) were loaded on 10-15% gradient SDS-PAGE gels.

Membranes were blocked (1h), incubated (2-16h) with primary antibody, washed, and incubated (1h) with HRP-conjugated secondary antibodies, all in blocking buffer (10 mM Tris-HCl, 150 mM NaCl, 0.1% Tween 20, pH 8.0; 5% non-fat dry milk). Membranes were washed (30 min) in blocking buffer without milk and briefly in 0.1% Tween 20 in PBS. HRP-conjugated antibodies were detected with ECL western blotting detection reagents (Amersham) according to the manufacturer's instructions. Antibody dilutions used are indicated in Supplementary Information, Table S1.

Gene expression analysis by RT-PCR

Total RNA was extracted using Invitrogen PureLink Micro-to-Midi Total RNA Purification System (Fig. 3; see Supplementary Information, Fig. S4) or a Qiagen RNeasy Minikit (Crawley, UK; Fig. 4), following the manufacturer's instructions. RNA (2 µg) was retrotranscribed with 50 ng Random primers and 10 U Reverse Transcriptase (Superscript II/III kit, Invitrogen) in a 20 µl reaction. The synthesized cDNA was diluted 1:10, and 2 µl were used for quantitative real-time PCR. Results are expressed relative to the appropriate control tissue, after normalization with *Gapdh*, *Ubc* and *G6PD* housekeeping genes. Primer sequences are available upon request.

FACS analysis

For Oct4 staining, ES-ERT2 cells were harvested by trypsinisation, washed in PBS and fixed (10 min, 37°C) in 0.1% paraformaldehyde in PBS.

Cells were washed in PBS and permeabilised (30 min, 4°C) with cold 90% methanol. After washing (2x) in PBS with 2% FCS and 0.1% Triton X-100, cells ($1-5 \times 10^5$) were incubated (1h) with anti-Oct4 antibody (Santa Cruz Biotechnology, N-19; 1:100). Cells were washed (2x) in PBS with 2% FCS and 0.1% Triton X-100 before incubating (30 min) with an AlexaFluor568-conjugated anti-goat IgG secondary antibody (Molecular Probes). Before analysis on a FACScalibur, the cells were washed (2x) in PBS with 1% BSA and 0.1% Triton X-100. The profile of Oct4 stained cells was compared to unstained cells and cells stained with the secondary antibody only.

For SSEA-1 staining, ES-ERT2 cells were harvested by trypsinisation using 0.05% Trypsin + 2% chicken serum and washed (3x) in PBS with 2% FCS. Cells ($1-5 \times 10^5$) were incubated (30-40 min, 4°C) in 35 μ l of APC-coupled anti-SSEA-1 (R&D: 1:3.5). Cells were washed (2x) in PBS with 2% FCS and analysed on a FACScalibur (BD Biosciences, Oxford, UK). SSEA-1 stained cells were compared to cells stained with APC-coupled non-relevant antibody (anti-B220).

Analysis of alkaline phosphatase activity

Cells were cultured (0 or 48h) in the presence of tamoxifen. After fixation, alkaline phosphatase activity was measured using a commercial kit, according to the manufacturer's instructions (Sigma, procedure 86). The stained colonies were imaged using a Leica (Milton Keynes, UK) MZ FLIII stereomicroscope with an 8x objective and a Leica DFC300 FX digital color camera.

Immunofluorescence

Asynchronous ES-ERT2 cells (1×10^5 cells) were plated on poly-L-lysine coated coverslips after 0 and 48 hours tamoxifen treatment to excise the *Ring1B* gene. Cells were fixed in 2% PFA (20 min, room temperature), washed 3x in PBS (3 min) and permeabilized in 0.4% Triton X-100 in PBS (5 min). Cells were then washed in PBS and in "wash" buffer (0.2% BSA, 0.05% Tween 20 in PBS), for 5 min and blocked in 2.5% BSA, 0.05% Tween 20, 10% NGS in PBS (30 min). Slides were washed once in wash buffer and incubated with Nanog antibody (1:100 in blocking buffer; 2h; Cosmo Bio Co.,

Ltd., Japan, REC-RCAB0002PF) in a humid chamber. Slides were washed in wash buffer (3x) and incubated with goat anti-rabbit secondary antibody, AlexaFluor488-conjugated (1:500 in blocking buffer; 45 min; Invitrogen) in a humid chamber. Slides were washed once with wash buffer and once in PBS and mounted in Vectashield containing DAPI. Cells were scored visually on a Leica DM IRBE epifluorescence microscope equipped with a 100x PL APO 1.40 oil objective. Images were collected sequentially on a confocal laser scanning microscope (Leica TCS SP5; 63x Plan APO 1.4 oil objective, NA 1.4, Milton Keynes, UK), equipped with a 405 diode and an Argon (488 nm) laser, and pinhole equivalent to 1 Airy disk. For comparison of Nanog staining during Ring1B depletion, images were collected on the same day using the same settings, and without saturation of the intensity signal. Raw TIFF images were merged in Adobe Photoshop (Adobe Systems, Edinburgh, UK) without further thresholding or filtering (e.g. no background subtraction).

Supplementary References

1. Billon, N., Jolicoeur, C., Ying, Q. L., Smith, A. & Raff, M. Normal timing of oligodendrocyte development from genetically engineered, lineage-selectable mouse ES cells. *J. Cell Sci.* **115**, 3657-3665 (2002).
2. Niwa, H., Miyazaki, J. & Smith, A. G. Quantitative expression of Oct-3/4 defines differentiation, dedifferentiation or self-renewal of ES cells. *Nat. Genet.* **24**, 372-376 (2000).
3. Mak, W. *et al.* Mitotically stable association of polycomb group proteins *eed* and *enx1* with the inactive X chromosome in trophoblast stem cells. *Curr. Biol.* **12**, 1016-1020 (2002).
4. Kunath, T. *et al.* Imprinted X-inactivation in extra-embryonic endoderm cell lines from mouse blastocysts. *Development* **132**, 1649-1661 (2005).
5. Szutorisz, H. *et al.* Formation of an active tissue-specific chromatin domain initiated by epigenetic marking at the embryonic stem cell stage. *Mol. Cell. Biol.* **25**, 1804-1820 (2005).
6. Azuara, V. *et al.* Chromatin signatures of pluripotent cell lines. *Nat. Cell Biol.* **8**, 532-538 (2006).
7. Daniel, T. & Carling, D. Functional analysis of mutations in the gamma 2 subunit of AMP-activated protein kinase associated with cardiac hypertrophy and Wolff-Parkinson-White syndrome. *J. Biol. Chem.* **277**, 51017-51024 (2002).
8. de Napoles, M. *et al.* Polycomb group proteins Ring1A/B link ubiquitylation of histone H2A to heritable gene silencing and X inactivation. *Dev. Cell* **7**, 663-676 (2004).
9. Kuzmichev, A., Nishioka, K., Erdjument-Bromage, H., Tempst, P. & Reinberg, D. Histone methyltransferase activity associated with a human multiprotein complex containing the Enhancer of Zeste protein. *Genes Dev.* **16**, 2893-2905 (2002).
10. Atsuta, T. *et al.* Production of monoclonal antibodies against mammalian Ring1B proteins. *Hybridoma* **20**, 43-46 (2001).
11. Chao, S. H. & Price, D. H. Flavopiridol inactivates P-TEFb and blocks most RNA polymerase II transcription in vivo. *J. Biol. Chem.* **276**, 31793-31799 (2001).
12. Lam, L. T. *et al.* Genomic-scale measurement of mRNA turnover and the mechanisms of action of the anti-cancer drug flavopiridol. *Genome Biol.* **2**, RESEARCH0041 (2001).
13. Arceci, R. J., King, A. A., Simon, M. C., Orkin, S. H. & Wilson, D. B. Mouse GATA-4: a retinoic acid-inducible GATA-binding transcription factor expressed in endodermally derived tissues and heart. *Mol Cell Biol* **13**, 2235-2246 (1993).
14. Singh, A. M., Hamazaki, T., Hankowski, K. E. & Terada, N. A Heterogeneous Expression Pattern for Nanog in Embryonic Stem Cells. *Stem Cells* **25**, 2534-2542 (2007).
15. Bernstein, B. E. *et al.* A bivalent chromatin structure marks key developmental genes in embryonic stem cells. *Cell* **125**, 315-326 (2006).